

Separating the signal from the noise: Evidence for deceleration in old-age death rates

Dennis M. Feehan
feehan@berkeley.edu

March 27, 2018

Abstract

Widespread population aging has made it critical to understand death rates at old ages. However, studying mortality at old ages is challenging because the data are sparse: numbers of survivors and deaths get smaller and smaller with age. We show how to address this challenge by using principled model selection techniques to empirically evaluate theoretical mortality models. We test nine different theoretical models of old-age death rates by fitting them to 360 high-quality datasets on cohort mortality above age 80. Models that allow for the possibility of decelerating death rates tend to fit better than models that assume exponentially increasing death rates. No single model is capable of universally explaining observed old-age mortality patterns, but the Log-Quadratic model most consistently predicts well. Patterns of model fit differ by country and sex; we discuss possible mechanisms, including sample size, period effects, and regional or cultural factors that may be important keys to understanding patterns of old-age mortality. We introduce a freely available R package that enables researchers to extend our analysis to other models, age ranges, and data sources.

1 Introduction

In the developed world, life expectancy at birth continues to rise and fertility levels are low. At the same time, much of the developing world has seen declines in birthrates and improvements in child and adult survival (United Nations Population Division 2015). Together, these trends have led demographers to forecast widespread and rapid population aging (Gerland et al. 2014). This shifting demographic landscape raises critical scientific and policy questions about the nature of human longevity (Kinsella et al. 2005; Martin and Preston 1994). To understand this phenomenon, researchers have proposed several different theories that aim to explain and predict patterns of death rates at advanced ages.¹ This study carefully assesses the amount of empirical support that these proposed theories have.

Understanding theoretical models of old-age mortality is important for several reasons. First, these models are critical to progress in answering a key question in the science of ageing: can we expect lifespans to increase indefinitely, or is there some upper limit at which our biology renders continued improvements essentially impossible (Dong et al. 2016; Lenart and Vaupel 2017)? To answer this question, researchers need evidence about empirical regularities in old-age death rates. Unfortunately, the sparse numbers of deaths at advanced ages has made establishing these empirical regularities quite difficult. For example, although it is widely accepted that death rates accelerate over the course of middle and early-old ages, there is less agreement about what happens to mortality at advanced ages: while some models of old-age mortality imply that death rates will continue to increase at oldest ages (Dong et al. 2016; Gompertz 1825; Makeham 1860), other models predict that death rates will decelerate or even plateau (L. A. Gavrilov and Gavrilova 2011; Horiuchi and Wilmoth 1998; A. Thatcher et al. 1998). Second, many policymakers and planners need accurate, mathematical summaries of death rates at advanced ages in order to produce forecasts and projections. For example, old-age mortality forecasts are a critical input to planning for health care and pension systems (Bongaarts 2005; Tabeau et al. 2001). Finally, understanding old-age survival patterns is important for a number of other research questions of great relevance to sociology, economics, and public policy. For example, a mathematical description of old-age mortality is needed to build a behavioral model of how increases in longevity are related to changes in savings and investment behavior (Sheshinski 2007).

The remainder of this article begins by briefly reviewing the theory behind nine leading models of old-age mortality (Section 2). We then introduce the dataset, which consists of high-quality information on population and deaths by age for 360 cohorts selected from the Kannisto-Thatcher database on old-age mortality (Section 3). Next, we discuss how to measure the relative amount of empirical support the various theories have (Section 4). This topic is critical because deaths at old ages are very rare, so careful attention must be paid to how models are fit and assessed. We then

¹In this paper, we use the term ‘advanced ages’ or ‘oldest ages’ to refer to ages over 80.

turn to a substantive analysis of the resulting model fits (Section 5). We find that models that allow for the possibility of decelerating death rates tend to fit better than models that assume continual exponential increase. The Log-Quadratic model performs best, but no single model can be said to adequately capture patterns of old-age mortality across all of the cohorts in our sample; instead, patterns of model fit vary considerably by country. We relate our findings to previous research and discuss several mechanisms that may be important determinants of old-age mortality patterns, including period effects, cultural factors, and country-specific differences in sample size. The paper concludes with a discussion and an outline of topics for future research (Section 6). As a companion to the article, we introduce a freely available R package that can be used to extend our analysis to other age ranges, models, and datasets.

2 Background and theory

2.1 Mortality models

Theoretical models of old-age mortality can be expressed in terms of (i) an individual hazard function and (ii) an aggregation method. Together, these two components lead to a *population hazard function* (Figure 1; Appendix B.1). For a group of people, the *population hazard function* is defined as:

$$\mu(z) = -\frac{d \log S(z)}{dz} = -\frac{1}{S(z)} \frac{dS(z)}{dz}. \quad (1)$$

where $S(z)$ is the *population survival function*, *i.e.* the proportion of group members that survives to exact age z .

Given a model for the population hazard, there is a mathematical relationship that links the hazard function $\mu(z)$ and the probability of dying between ages z and $z + k$, conditional on surviving to age z :

$$\pi(z, z + k) = 1 - \exp\left(-\int_z^{z+k} \mu(x) dx\right). \quad (2)$$

Equation 2 shows that a population hazard function can be converted into expected numbers of cohort deaths by age. A theory that has been expressed as a hazard function can thus be tested by comparing predicted numbers of deaths by age to empirically observed numbers of deaths by age.

Scientifically, it is important to understand both (1) how well a particular theory fits empirical data in an absolute sense; and (2) how well a theory fits empirical data *relative to other theories*.

Understanding how well a particular theory fits the data in an absolute sense is critical to its plausibility: a theory that is entirely inconsistent with empirical evidence must be discarded. Understanding how well a theory fits relative to other theories is critical to progress: even a theory that produces adequate fits to empirical data may be replaced by an alternate theory that consistently fits the data better. Relative comparisons of theories might also reveal that there is no consistent pattern to which theory fits data best, suggesting that multiple theories may have merit; that different theoretical mechanisms are important for different subgroups; or that adequate explanatory theories have not yet been proposed.

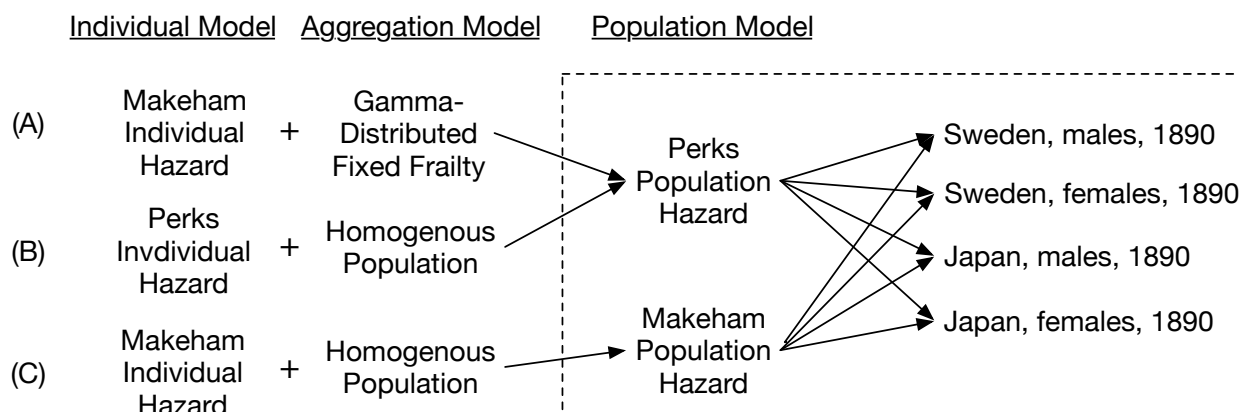


Figure 1: Illustrative example of three different possible mortality theories and their empirical predictions. The left-hand column shows different hazards that individuals might face. The next column shows examples of different ways that these individual hazards might aggregate up into the population hazard. Two different theoretical models, (A) and (B) lead to the same empirical prediction about cohort deaths by age (A. Yashin et al. 1994). Thus, models (A) and (B) cannot be distinguished without additional information. A third model, (C), makes a different empirical prediction. Thus, information on cohort deaths by age can be used to determine whether model (C) is better or worse than models (A) and (B). The dashed line shows what can be understood from analyzing cohort deaths by age, which is the focus of the analysis below.

2.2 Functional Forms for the Population Hazard

The most prominent models of old-age mortality have been expressed as hazard functions (Table 1). We now briefly review the theory associated with each of these models². These models can be described in four sets.

The first set contains models that can be considered generalizations of the Gompertz model. The Gompertz model is the oldest mathematical description of mortality; it was first proposed as a descriptive theory that could closely capture empirically observed risks of death, which increase rapidly across adult ages (Gompertz 1825). Researchers following Gompertz developed mechanism-

²Note that, although our focus is on old-age mortality, these models can also be applied to other age ranges.

based probability models that can produce Gompertzian mortality dynamics (Strehler and Mildvan 1960). Gompertz is considered to provide a good, stylized description of adult mortality throughout the middle to early-old age range, but some researchers argue that it fails to capture the dynamics of oldest-age mortality patterns (e.g., Vaupel et al. 1998). The Makeham model was designed to generalize the Gompertz model by adding a parameter that captures age-invariant ‘background’ mortality; this background mortality could, for example, describe everyone’s risk of death due to environmental factors that do not vary with age (Makeham 1860). The Log-Quadratic model has emerged from biodemographic investigations of lifespan and aging rates, and can be seen as a generalization of the Makeham model that adds a parameter which allows increases in death rates to decelerate at advanced ages (Coale and Kisker 1990; Steinsaltz and Wachter 2006; J. R. Wilmoth 1995).

The second set contains the Weibull model, which can be motivated by drawing analogies between human biology and theories of reliability rooted in engineering and manufacturing. These reliability theories describe systems composed of multiple components. Each component has some time-dependent risk of failure, independent of the other components (Weibull 1951). The Weibull model would make sense if, for example, the human body could be accurately modeled as a set of independent organs, with death resulting when any of the organs fails.

The third set contains the Logistic, Beard, Perks, and Kannisto models. These four models arose from research on heterogeneity in mortality; they result from postulating a distribution over individual hazard functions, leading to a population hazard that is a continuous mixture of these individual hazards (R. E Beard 1959; Perks 1932; Vaupel et al. 1979). For example, the Beard model can be derived by assuming that individuals face a Gompertz hazard and that each individual’s hazard has been scaled by a Gamma-distributed variate often called ‘frailty’ (R. E Beard 1959; Horiuchi and Wilmoth 1998; K. G. Manton et al. 1981). The Kannisto model is unique in this set because it was not derived from first principles; instead, it was proposed as a heuristic two-parameter approximation of the more complex heterogeneity models (Himes et al. 1994; A. Thatcher et al. 1998).

Finally, the fourth set contains the Lynch-Brown model, which was devised to describe and interpret observed crossovers in death rates between Black and White populations in the United States (S. M. Lynch and Brown 2001; Scott M. Lynch et al. 2003).

Table 1: The functional forms for the hazard of death at advanced ages considered in this analysis. In the functions listed above, z is age and $\mu(z)$ is the population hazard function. L. A Gavrilov and Gavrilova (1991) and A. Thatcher et al. (1998) contain helpful discussions about many of these functional forms.

Name	Parameters	Function	Sample references
Gompertz	α, β	$\mu(z) = \alpha \exp(\beta z)$	Gompertz (1825)

Name	Parameters	Function	Sample references
Kannisto	α, β	$\mu(z) = \frac{\alpha \exp(\beta z)}{1 + \exp(\beta z)}$	A. Thatcher et al. (1998)
Weibull	α, β	$\mu(z) = \alpha z^{\beta-1}$	Weibull (1951)
Makeham	α, β, γ	$\mu(z) = \gamma + \alpha \exp(\beta z)$	Makeham (1860)
Beard / Gamma-Gompertz	α, β, δ	$\mu(z) = \frac{\alpha \exp(\beta z)}{1 + \delta \exp(\beta z)}$	R. E Beard (1959), Horiuchi and Wilmoth (1998)
Log-Quadratic	α, β, γ	$\mu(z) = \exp(\alpha + \beta z + \gamma z^2)$	Coale and Kisker (1990), J. R. Wilmoth (1995) Steinsaltz and Wachter (2006)
Logistic	$\alpha, \beta, \gamma, \delta$	$\mu(z) = \gamma + \frac{\alpha \exp(\beta z)}{1 + \delta \exp(\beta z)}$	Perks (1932), Robert E. Beard (1971)
Perks / Gamma-Makeham	$\alpha, \beta, \gamma, \delta$	$\mu(z) = \frac{\gamma + \alpha \exp(\beta z)}{1 + \delta \exp(\beta z)}$	Perks (1932), R. E Beard (1959), Horiuchi and Wilmoth (1998)
Lynch-Brown	$\alpha, \beta, \gamma, \delta$	$\mu(z) = \alpha + \beta \arctan\{\gamma(z - \delta)\}$	S. M. Lynch and Brown (2001)

To recap: many theories have been proposed to explain the patterns of mortality at oldest ages. Each theory corresponds to a population hazard function which mathematically describes the predicted risk of death by age for a group of people. Population hazards can be converted into expected numbers of deaths by age, and predicted deaths by age can then be compared to observed deaths by age to determine how well each theory agrees with empirical evidence. Appendix E provides additional details and references to the literature.

3 Data

In order to empirically test the models in Table 1, we fit each model to data from the Kannisto-Thatcher (K-T) database on Old Age Mortality. The K-T database is a carefully curated collection of data on mortality at advanced ages, with information on deaths and exposure above age 80 for 35 countries, with some of the Scandinavian data going back to the mid-18th century (Kannisto

et al. 1994; MPIDR 2014). Since data quality for mortality at advanced ages is a serious concern (e.g., Black et al. 2017), we only analyze the subset of country-cohorts that were found to be of high quality by the expert review of Jdanov et al. (2008)³. Specifically, we retained the cohort data from all countries where more than half of the years were of the highest quality, and the remaining years were of the second-highest quality in the assessment the authors provided. Furthermore, we only selected countries and time periods where deaths were reported by single year of age up to 104. This leaves data from Denmark, France, West Germany, Italy, Japan, the Netherlands, Sweden, and Switzerland. In total, the analysis dataset has 360 cohorts of data on survivors and deaths by sex and single year of age from 10 different countries. Table 2 describes the years and cohorts in the analysis dataset, and Appendix A has more detail on how the analysis sample was chosen.

Table 2: Cohorts from the Kannisto-Thatcher Database on Old Age Mortality used in this analysis. Only cohorts with the highest-quality data and deaths reported at least up to age 105 by single year of age are included. The final dataset has data for 360 country-sex-cohorts from 10 countries. Jdanov et al. (2008) has a detailed discussion of data quality and Appendix A has more information about how the analysis dataset was constructed.

Country	Cohort start	Cohort end	Number of cohorts	Avg. size (80)	Avg. size (95)
Sweden	1821	1895	150	19,567	1,088
France	1866	1892	54	159,094	10,678
Netherlands	1871	1895	50	32,203	2,640
Denmark	1881	1895	30	16,836	1,478
Italy	1881	1895	30	159,915	10,872
West Germany	1891	1895	10	227,391	16,170
Japan	1891	1895	10	204,541	18,361
Scotland	1891	1895	10	18,258	1,468
Switzerland	1891	1895	10	21,349	2,021
Belgium	1893	1895	6	38,416	2,910

³Jdanov et al. (2008) developed methods to quantify several different ways that age patterns of deaths and population counts can be irregular. The researchers then systematically applied their methods to each cohort in the K-T database, producing comparable indicators for data quality across cohorts. Finally, Jdanov et al. (2008) summarized their results using hierarchical clustering, producing four tiers of data quality: best, acceptable, conditionally acceptable, and weak.

4 Methods

4.1 Likelihood and estimation

If N_z people from a cohort survive to exact age z , and all of the members of the cohort face the same hazard $\mu(z)$, then cohort deaths between exact ages z and $z + 1$ are distributed binomially:

$$D_z \sim \text{Binomial}(N_z, \pi(z, z + 1)),$$

where D_z is the number of deaths between ages z and $z + 1$, and $\pi(z, z + 1)$ is the probability of dying between ages z and $z + 1$ (Chiang 1960).

We fit each model to each cohort using the method of maximum likelihood. The likelihood for an observed sequence of deaths $\mathbf{D} = D_1, D_2, \dots$ and survivors to each age, $\mathbf{N} = N_1, N_2, \dots$ is then

$$Pr(\mathbf{D}|\mathbf{z}, \theta, \mathbf{N}) = \prod_z \binom{N_z}{D_z} \pi(z, \theta)^{D_z} (1 - \pi(z, \theta))^{(N_z - D_z)}. \quad (3)$$

Taking logs yields

$$ll(\mathbf{D}|\mathbf{z}, \theta, \mathbf{N}) = K + \sum_z [D_z \log(\pi(z, \theta)) + (N_z - D_z) \log(1 - \pi(z, \theta))], \quad (4)$$

where K is a constant that does not vary with θ . In order to fit a particular hazard model to a dataset (\mathbf{D}, \mathbf{N}) from a particular cohort, Equation 4 is maximized as a function of θ . The computation required to perform this maximization is not trivial; therefore, in Appendix B.2 and B.3 we provide a more detailed description of the methods we use to fit each cohort dataset and we introduce the freely available R package `mortfit` which other researchers can use to develop and fit their own mortality models⁴.

There are several advantages to fitting mortality hazards by building a likelihood-based model for the observed deaths by age. First, it is uncommon for people to survive to old ages, making absolute numbers of deaths and survivors small and rapidly decreasing by age. Fitting hazards using maximum likelihood naturally accounts for the amount of data available at each age; intuitively, older ages with fewer survivors and deaths have less information about likely parameter values, and thus less influence on parameter estimates than younger ages where lots of data are observed. A different approach, such as fitting a regression to observed central death rates, can result in

⁴We also make use of several R packages, including Daróczy and Tsegelskyi (2015), R Core Team (2014), H. Wickham (2009), Slowikowski and Irsson (2016), Schloerke et al. (2014), and H. Wickham et al. (2016).

parameter estimates that are heavily influenced by noisy observations at the oldest ages. Several studies have argued for the benefits of likelihood-based estimates of mortality models (K. G. Manton et al. 1981; Pletcher 1999; Promislow et al. 1999; Steinsaltz 2005; Wang et al. 1998). Second, fitting mortality hazards using likelihood-based inference enables the use of principled model selection techniques to help determine which model is most consistent with the data. The theory for one important technique, the AIC, relies upon likelihood-based inference. (Below, we discuss why these principled model selection techniques are important.) Finally, we model the counts of deaths by age because those are the data that are actually observed; modeling another quantity, such as central death rates, would require making additional assumptions.

4.2 Model selection

Now we turn to methods that can be used to assess how well each fitted model explains observed deaths in each cohort. One approach is to directly compare the observed number of deaths in a cohort to the model’s predicted number of deaths. For example, we can compute the sum of squared errors in the estimated number of deaths for each model-country-sex-year:

$$\text{SSE} = \sum_z \left(\hat{D}_z - D_z \right)^2, \tag{5}$$

where z ranges over the ages in the dataset. This quantity provides a natural measurement of each model’s *accuracy*—*i.e.*, how close each model’s predictions come to the observed numbers of deaths, in absolute terms.

The statistical literature on model selection has revealed that accuracy is only one of two important factors in assessing model fit. The second important factor is *generalizability*, which is the extent to which a model’s performance on the observed dataset can be expected to be replicated on future datasets that arise from the same data generating process. *Overfitting* is a crucial consideration here (Burnham and Anderson 2003; Claeskens and Hjort 2008). Models with many free parameters are more flexible, meaning that they can bend to fit the shape of observed patterns in the data; thus, models with many free parameters can be expected to fit any particular dataset closely. This flexibility could be advantageous or disadvantageous: a more flexible model would be able to capture more complex relationships between age and the risk of death; however, a more flexible model could also overfit—*i.e.*, a flexible model might pick up noisy artefacts due to small sample sizes at old ages.

Model selection techniques address the problem of overfitting by penalizing a model’s *complexity*—*i.e.*, the number of free parameters it has. Thus, model selection techniques trade off accuracy and model complexity. Since the SSE has no penalty for model complexity, models that overfit can nonetheless appear to perform very well according to SSE. In order to account for both model accuracy and

model generalizability, we evaluate model fits by focusing on an alternative metric called Akaike’s Information Criterion (AIC). The AIC is essentially a penalized log-likelihood, where the penalty is a function of the number of parameters being estimated in the model:

$$\text{AIC} = -2\mathcal{L} + 2k, \tag{6}$$

where \mathcal{L} is the value of the maximized likelihood from Equation 4, and k is the number of parameters being estimated. Although Equation 6 looks simple, it has been motivated by extensive theory. This theory shows that the AIC selects the candidate model that minimizes the expected Kullback-Leibler distance between the distribution of data implied by the model and the one that generated the data (Akaike 1974; Burnham and Anderson 2003; Claeskens and Hjort 2008). The derivation of the AIC reveals that the second term ($2k$) is a bias adjustment that corrects for overfitting; thus, the AIC results are an indication of how well each hazard function trades off the number of parameters estimated with the accuracy of its fit to the data.

The derivation of the AIC reveals that absolute AIC values are not interpretable; however, two models can be compared by examining the difference between their AICs. Thus, the results below focus on a quantity called ΔAIC . For a particular model fit, ΔAIC is the difference between (1) the AIC value attained by the model and (2) the AIC value obtained for the model that best fit the dataset. Thus, for the best-fitting model, ΔAIC is 0; for other models, ΔAIC will be greater than 0. The closer ΔAIC is to 0, the better its fit.

The results below focus on the AIC because it accounts for the tension between model complexity and accuracy; because it is motivated by rigorous statistical theory; and because it is widely used in the natural and social sciences. Alternative theoretical perspectives have been used to develop other principled model selection criteria. Appendix C describes two of these alternatives– the Bayesian Information Criterion and K -fold cross-validation– and compares the results based on the AIC to analogous results using these two alternative methods. We believe that the theory that motivates the AIC is most relevant to our goal in this study, but more detailed discussions of model selection, including comparisons between the AIC and BIC, can be found in Claeskens and Hjort (2008); Burnham and Anderson (2003); Burnham and Anderson (2004); Hoeting et al. (1999); Friedman et al. (2009); and Kass and Raftery (1995).

5 Results

Each model in Table 1 was fit separately for males and females in each cohort in Table 2. To build intuition, we first illustrate the results for a single cohort. Next, we examine the results for the entire dataset and for specific countries.

5.1 An illustrative example

Figure 2 shows the observed data and fitted models for Danish males born in 1895. The circles show the observed central death rates and the area of each circle is proportional to the number of person-years of exposure observed at each age. Figure 2 shows that there is much more information about the cohort’s mortality experience at age 80 than at age 100: by the oldest ages, the amount of data has diminished dramatically, meaning that the data contain relatively little information about the underlying mortality process at oldest ages. The curves in Figure 2 show the maximum likelihood fit of each model from Table 1. Some models apparently fit the observed data better than others: for example, the Lynch-Brown model is able to bend at oldest ages to account for what may be a deceleration in the observed central death rates, while the Gompertz model appears to be forced to forgo fitting the small amount of data at the highest ages in favor of closely fitting the majority of deaths, which are concentrated at earlier ages.

Table 3 shows several quantitative summaries of the fits shown in Figure 2. The models are ordered by the rank they attain using the AIC, where rank 1 is the model that fits the data the best. Table 3 also shows the log-likelihood, the sum of squared errors in the estimated number of deaths at each age (SSE), the SSE rank, and the difference between each model’s AIC and the minimum AIC (Δ AIC). According to the SSE the fitted deaths from Lynch-Brown model are closest to the observed deaths for this cohort. However, the four-parameter Lynch-Brown model is very flexible, and the SSE makes no adjustment to protect against overfitting. Table 3 shows the AIC—which penalizes each model’s complexity to guard against overfitting—suggests that the Kannisto model performs the best. Thus, although the Kannisto model is slightly less accurate than the Lynch-Brown model, this is compensated for by the fact that the Kannisto model uses only two parameters while the Lynch-Brown model uses four. The AIC suggests that if we saw more data from the same cohort, the fitted Kannisto model would be likely to fit this unseen data more accurately than the fitted Lynch-Brown model.

Table 3: Measurements of model fit for the cohort of Danish males born in 1895.

	log-likelihood	SSE	SSE rank	AIC	AIC rank	Δ AIC
Kannisto	-29092.2	7645.48	6	58188.43	1	0
Beard	-29092.1	7645.43	3	58190.12	2	1.7
Log-Quadratic	-29092.1	7645.45	5	58190.25	3	1.8
Gompertz	-29093.4	7645.81	8	58190.76	4	2.3
Lynch-Brown	-29092	7645.39	1	58192.06	5	3.6
Logistic	-29092	7645.42	2	58192.09	6	3.7
Perks	-29092.1	7645.44	4	58192.2	7	3.8

	log-likelihood	SSE	SSE rank	AIC	AIC rank	Δ AIC
Makeham	-29093.4	7645.81	7	58192.76	8	4.3
Weibull	-29154.8	7656.04	9	58313.55	9	125

5.2 Results for all cohorts

Figure 3 shows boxplots that summarize the distribution of Δ AIC across all 360 cohorts, by sex. Note that these results essentially weight the mortality experience of each country by the number of cohorts that it contributes to the sample (Table 2). Several observations emerge from this figure: first, according to the median Δ AIC value, no single model clearly performs the best; instead, several of the models have very similar performance: for example, across both sexes, the Log-Quadratic, Beard, and Kannisto models have the lowest median Δ AIC values, and those median Δ AIC values are all very close to one another. Second, Figure 3 shows that there is much more variation in Δ AIC for some models than there is for others; for example, the interquartile range in Δ AIC across female cohorts is 2 for the Perks model, while it is 15 for the Kannisto model. The Weibull model consistently performed poorly, so we do not discuss it further.

The variation in Δ AIC (Figure 3) reveals that there is more than one factor to consider when evaluating the fit of each model. It is desirable to find a model that (1) often fits the data well and (2) rarely fits the data poorly. Burnham and Anderson (2003) propose rules of thumb that can help interpret Δ AIC with these two goals in mind: models with ‘substantial support’ from the data have Δ AIC ≤ 2 while models with ‘essentially no support’ from the data have Δ AIC > 10 (Burnham and Anderson 2003, pg. 72). Figure 4 uses these rules of thumb to compare the fraction of cohorts for which each model fits the data well (x axis) and the fraction of cohorts for which each model fits the data poorly (y axis). Several observations can be made about Figure 4. First, according to Δ AIC the Log-Quadratic model appears to come closest to satisfying the two goals: it often fits the data well (Δ AIC ≤ 2 for more than three quarters of cohorts) and it rarely fits the data poorly (Δ AIC > 10 for fewer than one tenth of cohorts); the Beard model performs almost as well as Log-Quadratic. Second, several models that do not fit the data extremely well also avoid fitting the data extremely badly. In particular, the most flexible models— Perks, Logistic, and Lynch-Brown—do not often fit the data the best (all have Δ AIC ≤ 2 for less than half of the cohorts), but these four-parameter models also rarely fit the data very poorly (all have Δ AIC > 10 for less than one tenth of the cohorts). Finally, Figure 4 reveals that most of the patterns of model fit are very similar for male and for female cohorts. There are three notable exceptions: the Kannisto, Gompertz, and Makeham models all show bigger differences between the fits for males and females than the other models do. For all three of these models, the point on Figure 4 summarizing fits to male cohorts is below and to the right of the point summarizing fits to female cohorts; thus, the

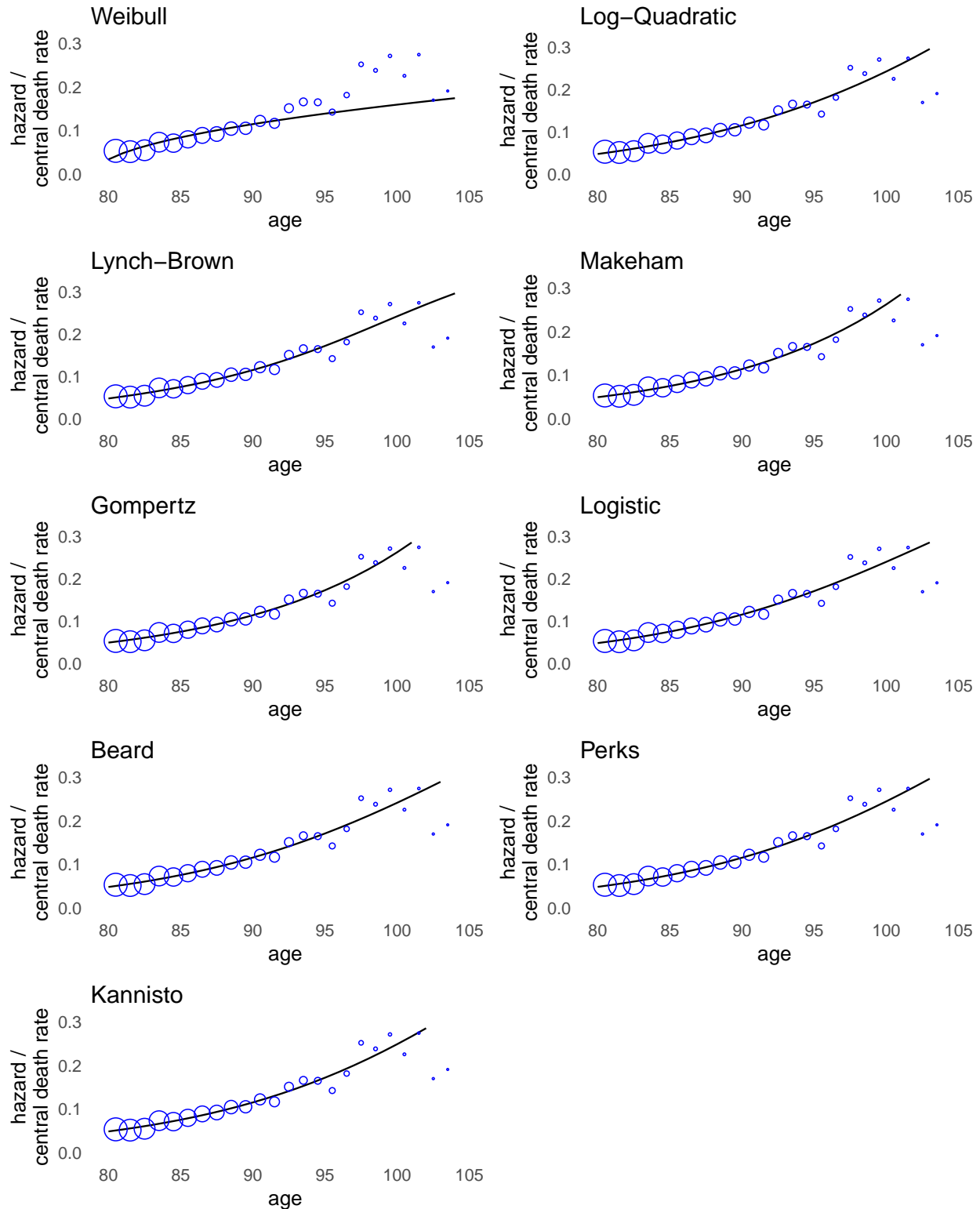


Figure 2: Models fit to the cohort data for Danish males born in 1895. The circles show the observed central death rates, the area of each blue circle is proportional to the estimated person-years of exposure at each age, and the curves show the maximum likelihood fit of each model. Quantitative summaries of goodness of fit are shown in Table 3. The AIC suggests that the Kannisto model best fits this cohort.

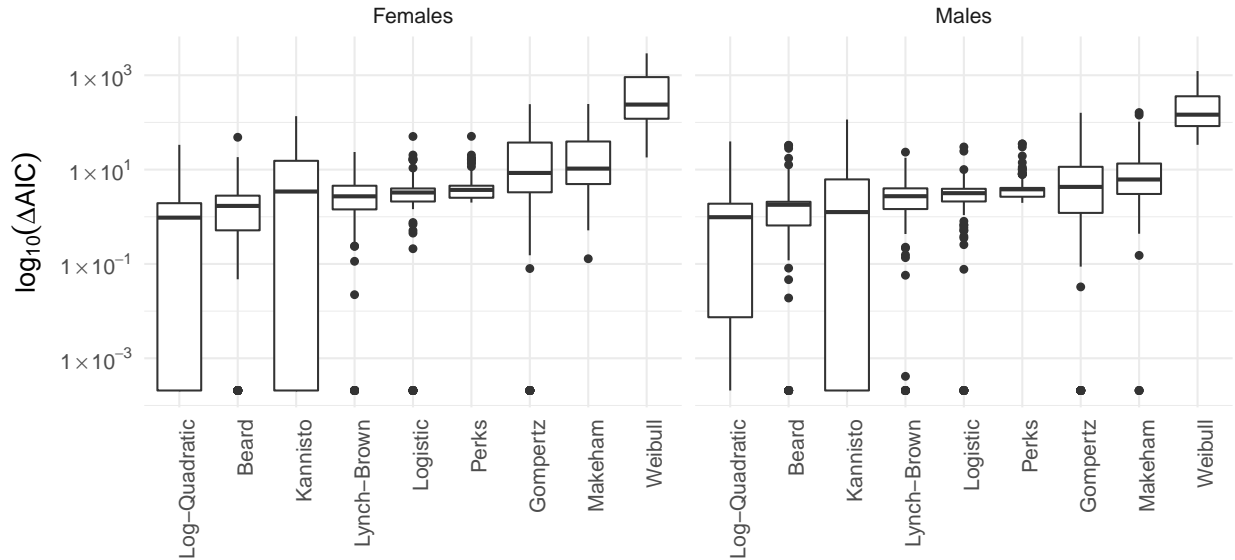


Figure 3: Boxplots summarizing the distributions of ΔAIC across all of the cohorts in the sample (note that the y axis is on a log scale). For each box, the horizontal line shows the median, the edges of the box show the interquartile range, and the whiskers extend to the largest and smallest values within 1.5 times the interquartile range; more extreme points are plotted separately. The Log-Quadratic, Beard, and Kannisto models appear to perform the best.

Gompertz, Makeham, and Kannisto models systematically do a better job of capturing the patterns in male mortality than female mortality.

Next, we investigate the possibility that there are pairs or groups of models that tend to perform relatively well or to perform relatively poorly for the same cohorts. Figure 5 shows a dendrogram that describes the similarity between patterns of ΔAIC for each model across all 360 cohorts⁵. Figure 5 suggests that a natural grouping can be obtained by picking a dissimilarity of about 200, which results in three groups of models: the first group contains the Log-Quadratic, Perks, Beard, Logistic, and Lynch-Brown models; the second group contains the Kannisto model; and the third group contains the Gompertz and Makeham models. Figure 3 and Figure 4 show that models from the first group—which consists of functional forms that can bend to accommodate decelerating death rates at older ages—tend to fit the data well: they rarely have $\Delta\text{AIC} \geq 10$, and the Log-Quadratic and Beard models have the highest fraction of cohorts with $\Delta\text{AIC} < 2$. In the second group, the Kannisto model’s relative performance is more ambiguous because there is a large amount of variance in the quality of its fits; for some cohorts, Kannisto performs as well as models from the first group, but for other cohorts, Kannisto’s performance is more similar to the Gompertz/Makeham models. Finally, in the third group, the Gompertz and Makeham models

⁵The distance metric used in Appendix Figure 5 is group average difference in ΔAIC values. Friedman et al. (2009) has more details on hierarchical clustering.

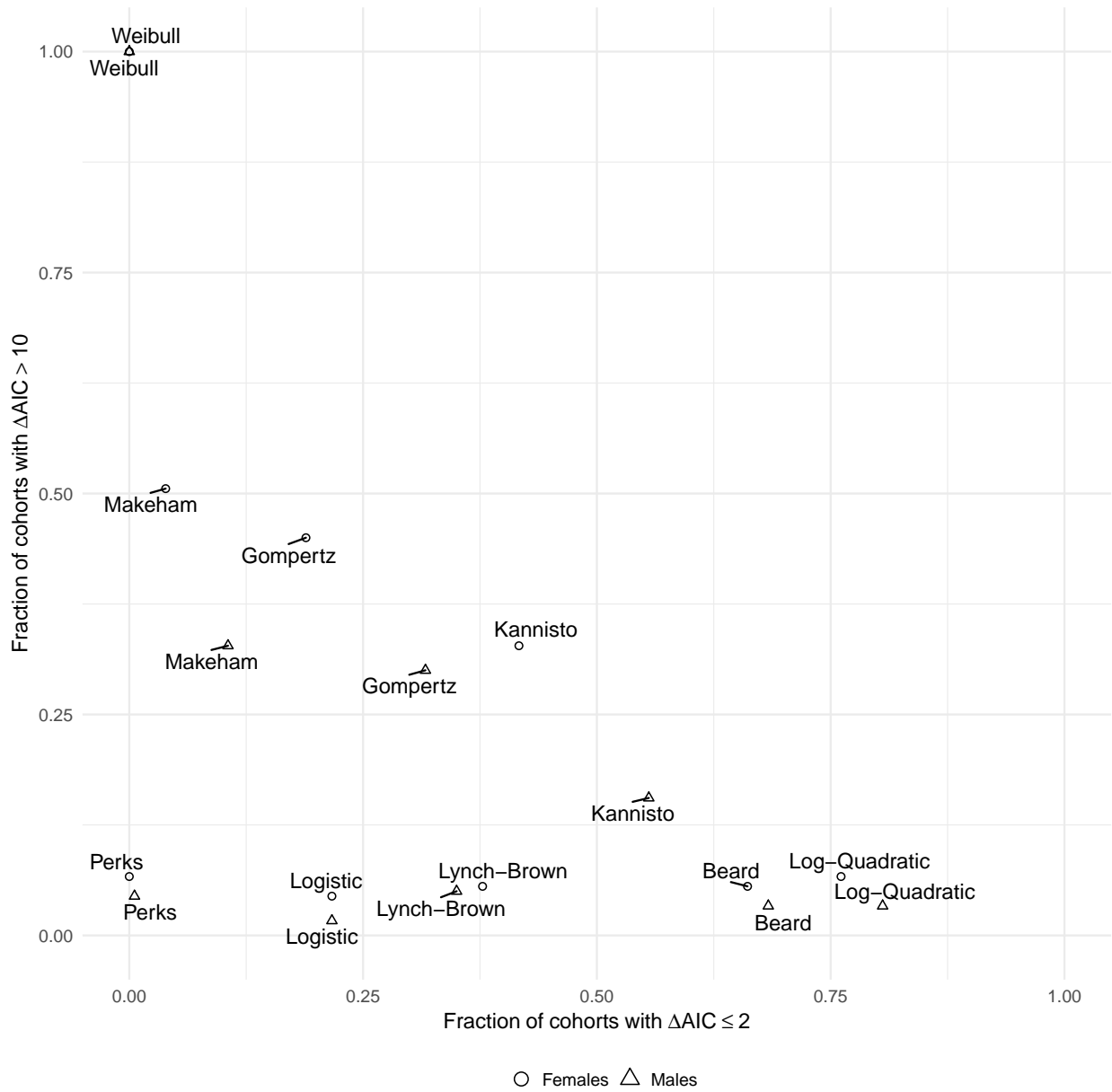


Figure 4: Fraction of cohorts for which the fit of each model had substantial support ($\Delta AIC \leq 2$, x axis) compared to the fraction of cohorts for which the fit of each model had essentially no support ($\Delta AIC > 10$, y axis). Models in the lower-right corner consistently fit the cohorts in the sample well; models in the lower-left corner are neither very good nor very bad; models in the upper-left corner consistently fit the cohorts in the sample poorly.

clearly tend to perform worse than the more flexible models in the first group, suggesting that the steady exponential increase in death rates observed at middle adult ages tends not to continue into advanced ages.

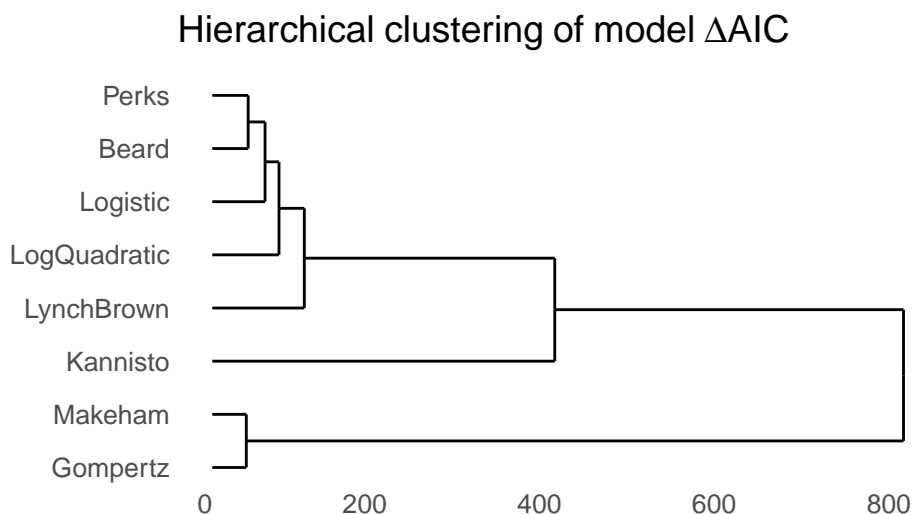


Figure 5: Dendrogram showing the relationship between model ΔAIC across all of the cohorts in our sample. The Weibull model was omitted, since it provides uniformly poor fits.

Each node in the tree corresponds to a clustering of models into two groups, one given by the tree corresponding to the node’s top child and one to the tree corresponding to the node’s bottom child. The position of the node along the x axis is proportional to the dissimilarity in between the two clusters; this dissimilarity is calculated as the Euclidean distance between the two cluster averages. The entire dendrogram shows a nested sequence of clusterings, called a *hierarchical clustering*; picking any dissimilarity value on the x axis produces a clustering.

5.3 Results by country

The results in Section 5.2 summarize model fits across the entire sample, which consists of cohorts from many different countries. We now turn to an analysis of model fits within each country, focusing on the five countries where more than 10 cohorts are observed for each sex: Denmark, France, Italy, the Netherlands, and Sweden. The remaining five countries—Belgium, West Germany, Japan, Scotland, and Switzerland—had 10 or fewer cohorts each; to avoid the risk of making misleading inferences from so few cohorts, we omit them from this country-specific analysis.

Figure 6 again uses the rules of thumb to show the fraction of cohorts for which each model has considerable support (x axis) and the fraction of cohorts for which each model has essentially no support (y axis) within each country and sex.⁶ The results suggest that (1) there are big differences in how the models fit cohorts from different countries, but (2) within each country there tend not to

⁶The figure omits the Weibull model, which consistently fit poorly across all countries (Figure 4).

be big differences in model fits by sex. The performance of the Gompertz and the Makeham models distinguishes countries from one another: in France and Italy, the Gompertz and Makeham models clearly perform poorly, and more flexible models fit well. For Denmark, the Gompertz and Makeham models do not rank at the top, but they rarely predict death rates very poorly ($\Delta\text{AIC} > 10$ in few cohorts). Sweden and the Netherlands are intermediate cases where Gompertz and Makeham predict poorly under half of the time.

5.4 Summary and Discussion

The Gompertz model provides a remarkably good description of death rates at young and middle adult ages, and researchers have long debated whether or not Gompertzian increases in death rates continue indefinitely with age (*e.g.* Bebbington et al. 2014; Olshansky and Carnes 1997; A. Thatcher et al. 1998; Vaupel et al. 1998). A key finding of our analysis is that flexible, non-Gompertzian models tend to fit old-age death rates better than Gompertz models in our sample of 360 high-quality cohorts from the Kannisto-Thatcher database⁷. This finding supports the idea that death rates tend to decelerate at oldest ages. Critically, we reached this conclusion by using a principled approach to model selection which accounted for the fact that there are very small numbers of deaths at advanced ages.

Our findings are consistent with several previous studies that have uncovered evidence of non-Gompertzian patterns in old-age death rates using other methods or data sources (Horiuchi and Wilmoth 1998; A. Thatcher et al. 1998; Vaupel et al. 1998; Yi and Vaupel 2003). However, recent analyses have also found support for Gompertz-type models of old-age mortality in some cases. Bebbington et al. (2014) used the Human Mortality Database to find that old-age mortality patterns for most countries do not follow a Gompertz-type trajectory; however, Bebbington et al. (2014) identified three notable exceptions where the Gompertz model fit well: Australia, Canada, and the United States. This raises the possibility that there may be a group of countries for which the Gompertz model provides a good description of old-age mortality. So far, this hypothesis has mixed support: in the United States, L. A. Gavrilov and Gavrilova (2011) and N. S. Gavrilova and Gavrilov (2015) analyzed the US Social Security Death Master File and found additional evidence supporting Gompertzian old-age mortality in the US. In Canada, however, Ouellette (2016) finds non-Gompertz mortality trajectories in old-age mortality among French Canadians in Quebec. Further, recent research in actuarial modeling suggests that non-Gompertzian dynamics may appear in Australian old-age mortality (J. S. H. Li et al. 2011). Thus, recent studies support the suggestion that US old-age mortality dynamics may be Gompertzian, but there are mixed results for Australia and Canada. Our study cannot directly address the debate in these three countries, since the

⁷Appendix C shows that this conclusion is robust to the choice of AIC, BIC, or cross-validation as the principled model fit technique.

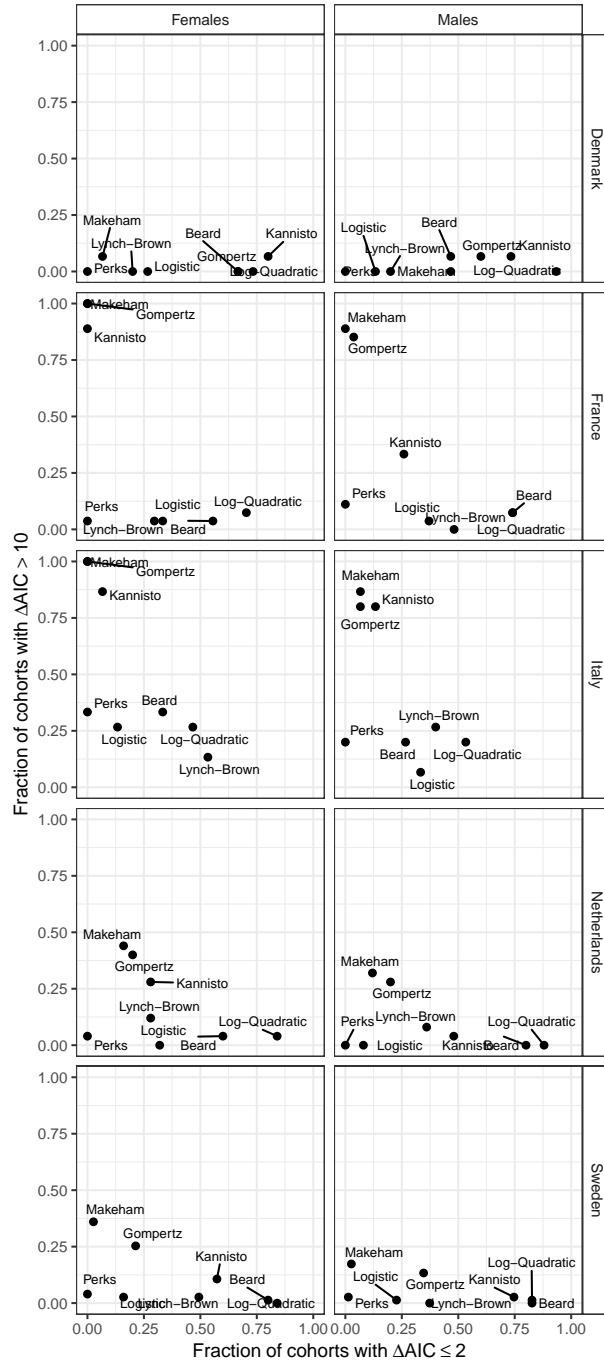


Figure 6: Fraction of cohorts for which the fit of each model had substantial support ($\Delta AIC \leq 2$, x axis) compared to the fraction of cohorts for which the fit of each model had essentially no support ($\Delta AIC > 10$, y axis) for each sex and for each country with at least ten cohorts of data. Models in the lower-right corner consistently fit the cohorts in the sample well; models in the lower-left corner are neither very good nor very bad; models in the upper-left corner consistently fit the cohorts in the sample poorly.

Kannisto-Thatcher data from Australia, Canada, and the United States were not of the highest quality, and so they were excluded from this analysis.

Although we are able to conclude that flexible models from the first group tend to perform better than the Gompertz/Makeham models in the third group, our results do not support the idea that any particular one of these nine models universally describes old-age mortality. The Log-Quadratic model most frequently provided accurate fits, but even the Log-Quadratic only had substantial support from the data ($\Delta\text{AIC} \leq 2$) in about three quarters of the cohorts studied; thus, even the Log-Quadratic model cannot be said to comprehensively capture all of the patterns in our sample.

We also found that patterns of model fit differed by country. Models from the Gompertz group did not reliably fit well ($\Delta\text{AIC} < 2$) in any of the countries; however, countries can be differentiated according to the fraction of cohorts in which the Gompertz group models performed poorly ($\Delta\text{AIC} > 10$). France and Italy stand out because in these two countries models from the Gompertz group were clearly inadequate: they did not often fit well, and frequently fit poorly⁸. Sweden and the Netherlands are intermediate cases in which models from the Gompertz group tended not to provide the best fit, but the Gompertz group models only performed poorly for about half of the cohorts. Finally, in Denmark models from the Gompertz group tended not to provide the best fit, but performed the best among the countries considered here. (In Denmark, none of the models consistently performed poorly.)

There are several possible explanations for these differing patterns by country, and these explanations are not mutually exclusive. First, it is possible that relatively large cohort sizes in Italy and France provide enough statistical power to detect deviations from Gompertzian dynamics, while smaller cohort sizes in Denmark, Sweden, and the Netherlands make this more difficult, even if underlying mortality dynamics in the smaller countries are non-Gompertzian. Although this possibility seems compelling, initial investigations revealed that artificially sampling successively smaller cohort sizes from the French data did not automatically lead to better performance by the Gompertz models, but instead tended to eventually produce better performance by the Kannisto model (Appendix D). Thus, although sample size is clearly a factor in our ability to detect deviations from non-Gompertzian mortality dynamics, it seems unlikely that it is the only explanation for the country-specific patterns reported here.

Second, it is possible that country-specific differences in the timing and rate of change of death rates at oldest ages leads to different patterns of fit by country. This view is supported by the fact that the country groupings suggested by our analysis are consistent with previous studies of levels and changes in adult mortality in Europe: other researchers have observed a contrast between Southern European countries like France and Italy, which showed continual improvement in adult death

⁸This finding that France and Italy do not fit Gompertzian old-age mortality patterns is confirmed even when other methods of assessing model fit, based on different statistical theories, are considered (Appendix C).

rates since the middle of the twentieth century, and some Northern European countries, including Denmark and the Netherlands, whose adult mortality gains have been less even, with periods of relative stagnation (Luy et al. 2011; Meslé and Vallin 2006; R. Rau et al. 2008). Staetsky (2009) argues that these contrasting patterns in female mortality change can be explained by differences in the timing and intensity of smoking, with women in Denmark and the Netherlands starting to smoke in earlier time periods than their counterparts in Italy and France. Interestingly, Staetsky (2009) points out that the timing of smoking in Denmark and the Netherlands closely follows the trend in the United States, a country where Bebbington et al. (2014) and L. A. Gavrilov and Gavrilova (2011) found support for Gompertz patterns of old-age mortality. Thus, our country-specific results suggest that period effects may have altered the shape of cohort mortality, so that cohorts that experienced continual improvements (France and Italy) show the strongest evidence of non-Gompertz death rates.

Third, these country-specific differences in model fits could be the result of more fundamental differences in the mortality regime of each country. These differences could be produced by country-specific differences in genetic or cultural factors—such as patterns of diet, physical activity, and social support—that are known to be important predictors of adult mortality and are thus likely to be moderators of old-age mortality (Berkman and Syme 1979; Byberg et al. 2009; Gjonca et al. 2000; Haveman-Nies et al. 2003; Vaupel et al. 2003).

Finally, we examined patterns of model fit by sex. Across all cohorts, most models showed similar performance for males and for females. The exceptions were the Gompertz, Makeham, and Kannisto models, which systematically tended to fit male cohorts better than female cohorts (Figure 4). More generally, patterns of model fit varied more across countries than across sexes; this finding was somewhat surprising, since adult mortality levels are often found to be more similar among cohorts of the same sex from different countries, as opposed to cohorts of different sexes from the same country (e.g., Fig. 3.4 in Luy et al. 2011). We consider understanding this finding an important topic for future research.

6 Conclusion

These results lead us to offer some suggestions for researchers who wish to model old-age mortality in the future. First, researchers who develop and fit mortality models should use a principled model selection technique like the AIC to assess model fit. Second, if a single model is to be used to model old-age mortality hazards, our results suggest that the Log-Quadratic model is a reasonable choice. Other models can also perform well, though our results showed that the Kannisto model—which is often used in practice—should be chosen with caution. Finally, our results suggest that researchers should be cautious about designing mortality studies that exclusively use data from only one country,

particularly if cohort sizes from the country tend to be small.

This study has several limitations and the results suggest several directions for future research. Any study of old-age mortality is limited by the quantity and quality of data available. We restricted our analysis to cohorts in the Kannisto-Thatcher database that have been identified as having the highest quality data, but it is possible that some inaccuracies remain. Severe data inaccuracies could affect model fits and thus our conclusions.

More generally, like many analyses of old-age mortality, we are restricted to analyzing groups of people that have been defined by political boundaries (i.e. countries). This approach is reasonable because people who live in the same country are governed by the same national policy regime; further, people who live in the same country may tend to be genetically similar and may tend to live in similar cultural environments. However, there can be a great deal of variation within a single country. Most models of mortality—even those models that explicitly account for heterogeneity—are most appropriate for one *coherent* population whose members face some continuous distribution of hazards. Countries that are big and diverse may well be better described as finite mixtures of coherent populations. Thus, it may be productive to try to construct datasets for cohorts whose members are most likely to share a common characteristic mortality experience, possibly with individual variation.

Our design focused on analyzing high-quality information on deaths and exposure for entire cohorts. Other designs based on collecting more detailed information from samples of people—such as longitudinal health surveys that link respondents to death certificate data—should also be used to assess the empirical support for different theories of old-age mortality. These designs have many advantages, as well as a different set of methodological and data quality challenges; thus, longitudinal surveys can be seen as an important complement to the analysis here.

Finally, we hope this analysis can be a helpful starting point for building more complex models to understand and to forecast old-age mortality. Future work could investigate how to combine these theoretical models into predictive ensembles; researchers could also build a hierarchical model that describes how cohorts in the sample are related to one another. Either or both of these approaches could be used to stochastically forecast future old-age death rates.

7 References

- Abramowitz, M., & Stegun, I. A. (1964). *Handbook of mathematical functions: With formulas, graphs, and mathematical tables* (Vol. 55). Courier Corporation.
- Akaike, H. (1974). A new look at the statistical model identification. *IEEE transactions on automatic control*, *19*(6), 716–723.
- Beard, R. E. (1959). Appendix: Note on Some Mathematical Mortality Models, 302–311.
- Beard, R. E. (1971). Some aspects of theories of mortality, cause of death analysis, forecasting and stochastic processes. *Biological aspects of demography*, 57–68.
- Bebbington, M., Green, R., Lai, C.-D., & Zitikis, R. (2014). Beyond the Gompertz law: Exploring the late-life mortality deceleration phenomenon. *Scandinavian Actuarial Journal*, *2014*(3), 189–207.
- Berkman, L. F., & Syme, S. L. (1979). Social networks, host resistance, and mortality: A nine-year follow-up study of Alameda County residents. *American Journal of Epidemiology*, *109*(2), 186–204.
- Black, D. A., Hsu, Y.-C., Sanders, S. G., Schofield, L. S., & Taylor, L. J. (2017). *The Methuselah Effect: The Pernicious Impact of Unreported Deaths on Old Age Mortality Estimates*. National Bureau of Economic Research.
- Bongaarts, J. (2005). Long-range trends in adult mortality: Models and projection methods. *Demography*, *42*(1), 23–49.
- Burnham, K. P., & Anderson, D. (2003). Model selection and multi-model inference: A practical information-theoretic approach. *Springer*.
- Burnham, K. P., & Anderson, D. R. (2004). Multimodel Inference: Understanding AIC and BIC in Model Selection. *Sociological Methods & Research*, *33*(2), 261–304.
- Byberg, L., Melhus, H., Gedeberg, R., Sundström, J., Ahlbom, A., Zethelius, B., et al. (2009). Total mortality after changes in leisure time physical activity in 50 year old men: 35 year follow-up of population based cohort. *BMJ*, *338*, b688.
- Chiang, C. L. (1960). A stochastic study of the life table and its applications: I. Probability distributions of the biometric functions. *Biometrics*, *16*(4), 618–635.
- Claeskens, G., & Hjort, N. L. (2008). *Model selection and model averaging* (Vol. 330). Cambridge University Press Cambridge.
- Coale, A. J., & Kisker, E. E. (1990). Defects in data on old-age mortality in the United States: New procedures for calculating mortality schedules and life tables at the highest ages.

- Daróczi, G., & Tsegelskyi, R. (2015). *Pander: An R Pandoc Writer*. R package version 0.6.0.
- Dong, X., Milholland, B., & Vijg, J. (2016). Evidence for a limit to human lifespan. *Nature*, *538*(7624), 257–259.
- Efron, B., & Hastie, T. (2016). *Computer Age Statistical Inference* (Vol. 5). Cambridge University Press.
- Friedman, J., Hastie, T., & Tibshirani, R. (2009). The Elements of Statistical Learning: Data Mining, Inference, and Prediction. *Springer Series in Statistics*.
- Gavrilov, L. A., & Gavrilova, N. S. (1991). *The biology of life span: A quantitative approach*. Chur [Switzerland]; New York: Harwood Academic Publishers.
- Gavrilov, L. A., & Gavrilova, N. S. (2011). Mortality measurement at advanced ages: A study of the Social Security Administration Death Master File. *North American actuarial journal: NAAJ*, *15*(3), 432.
- Gavrilova, N. S., & Gavrilov, L. A. (2015). Biodemography of Old-Age Mortality in Humans and Rodents. *The Journals of Gerontology: Series A*, *70*(1), 1–9.
- Gerland, P., Raftery, A. E., Ševčíková, H., Li, N., Gu, D., Spoorenberg, T., et al. (2014). World population stabilization unlikely this century. *Science*, *346*(6206), 234–237.
- Gjonca, A., Maier, H., & Brockmann, H. (2000). Old-Age Mortality in Germany prior to and after Reunification. *Demographic Research*, *3*.
- Gompertz, B. (1825). On the Nature of the Function Expressive of the Law of Human Mortality, and on a New Mode of Determining the Value of Life Contingencies. *Philosophical Transactions of the Royal Society of London*, *115*, 513–583.
- Haveman-Nies, A., Groot, D., C.p.g.m, L., Staveren, V., & A, W. (2003). Dietary quality, lifestyle factors and healthy ageing in Europe: The SENECA study. *Age and Ageing*, *32*(4), 427–434.
- Himes, C., Preston, S., & Condran, G. (1994). A relational model of mortality at older ages in low mortality countries. *Population Studies*, *48*(2), 269–291.
- Hoeting, J. A., Madigan, D., Raftery, A. E., & Volinsky, C. T. (1999). Bayesian model averaging: A tutorial. *Statistical science*, 382–401.
- Horiuchi, S. (2003). Interspecies differences in the life span distribution: Humans versus invertebrates. *Population and Development Review*, *29*, 127–151.
- Horiuchi, S., & Wilmoth, J. R. (1998). Deceleration in the age pattern of mortality at older ages. *Demography*, *35*(4), 391–412.

- Jdanov, D. A., Jasilionis, D., Soroko, E. L., Rau, R., & Vaupel, J. W. (2008). Beyond the Kannisto-Thatcher Database on Old-Age Mortality: An assessment of data quality at advanced ages. *MPIDR Working Papers*.
- Kannisto, V., Lauritsen, J., Thatcher, A. R., & Vaupel, J. W. (1994). Reductions in mortality at advanced ages: Several decades of evidence from 27 countries. *Population and Development Review*, 793–810.
- Kass, R. E., & Raftery, A. E. (1995). Bayes Factors. *Journal of the American Statistical Association*, 90(430), 773–795.
- Kinsella, K., Phillips, D., & Bureau, P. R. (2005). *Global aging: The challenge of success*. Population Reference Bureau.
- Le Bras, H. (1976). Lois de mortalité et age limite. *Population (French Edition)*, 655–692.
- Lenart, A., & Vaupel, J. W. (2017). Questionable evidence for a limit to human lifespan. *Nature*, 546(7660), E13.
- Li, J. S. H., Ng, A. C. Y., & Chan, W. S. (2011). Modeling old-age mortality risk for the populations of Australia and New Zealand: An extreme value approach. *Mathematics and Computers in Simulation*, 81(7), 1325–1333.
- Luy, M., Wegner, C., & Lutz, W. (2011). Adult mortality in Europe. In *International handbook of adult mortality* (pp. 49–81). Springer.
- Lynch, S. M., & Brown, J. S. (2001). Reconsidering mortality compression and deceleration: An alternative model of mortality rates. *Demography*, 38(1), 79–95.
- Lynch, S. M., Brown, J. S., & Harmsen, K. G. (2003). Black-White Differences in Mortality Compression and Deceleration and the Mortality Crossover Reconsidered. *Research on Aging*, 25(5), 456–483.
- Makeham, W. M. (1860). On the law of mortality and the construction of annuity tables. *The Assurance Magazine, and Journal of the Institute of Actuaries*, 301–310.
- Manton, K. G., Stallard, E., & Vaupel, J. W. (1981). Methods for comparing the mortality experience of heterogeneous populations. *Demography*, 18(3), 389–410.
- Manton, K. G., Stallard, E., & Vaupel, J. W. (1986). Alternative models for the heterogeneity of mortality risks among the aged. *Journal of the American Statistical Association*, 81(395), 635–644.
- Martin, L., & Preston, S. (1994). *Demography of aging*. National Academies Press.

Meslé, F., & Vallin, J. (2006). Diverging Trends in Female Old-Age Mortality: The United States and the Netherlands versus France and Japan. *Population and Development Review*, 32(1), 123–145.

MPIDR. (2014). Kannisto-Thatcher Database on Old-Age Mortality. <http://www.demogr.mpg.de/databases/ktdb/>

Nocedal, J., & Wright, S. (1999). *Numerical optimization*. Springer Verlag.

Olshansky, S. J., & Carnes, B. A. (1997). Ever since Gompertz. *Demography*, 34(1), 1–15.

Ouellette, N. (2016). La forme de la courbe de mortalité des centenaires canadiens-français. *Gérontologie et société*, 39(3), 41–53.

Perks, W. (1932). On some experiments in the graduation of mortality statistics. *Journal of the Institute of Actuaries*, 12–57.

Pletcher. (1999). Model fitting and hypothesis testing for age-specific mortality data. *Journal of Evolutionary Biology*, 12(3), 430–439.

Preston, S., Heuveline, P., & Guillot, M. (2000). *Demography: Measuring and modeling population processes*.

Promislow, Tatar, Pletcher, & Carey. (1999). Below-Threshold mortality: Implications for studies in evolution, ecology and demography. *Journal of Evolutionary Biology*, 12(2), 314–328.

R Core Team. (2014). *R: A language and environment for statistical computing*. Vienna, Austria: R Foundation for Statistical Computing.

Rau, R., Soroko, E., Jasilionis, D., & Vaupel, J. W. (2008). Continued Reductions in Mortality at Advanced Ages. *Population and Development Review*, 34(4), 747–768.

Schloerke, B., Crowley, J., Cook, D., Hofmann, H., Wickham, H., Briatte, F., et al. (2014). *GGally: Extension to ggplot2. R package version 0.5. 0*.

Sheshinski, E. (2007). *The Economic Theory of Annuities*. Princeton University Press.

Slowikowski, K., & Irisson, J. (2016). *Ggrepel: Repulsive Text and Label Geoms for ggplot2. R package version 0.6. 5*.

Staetsky, L. (2009). Diverging trends in female old-age mortality: A reappraisal. *Demographic Research; Rostock*, 21, 885–914.

Stein, W. (2008). Sage: Open source mathematical software. 7 December 2009.

Steinsaltz, D. (2005). Re-evaluating a test of the heterogeneity explanation for mortality plateaus. *Experimental gerontology*, 40(1-2), 101–113.

- Steinsaltz, D., & Wachter, K. (2006). Understanding Mortality Rate Deceleration and Heterogeneity. *Mathematical Population Studies*, 13(1), 19–37.
- Stone, M. (1977). An asymptotic equivalence of choice of model by cross-validation and Akaike's criterion. *Journal of the Royal Statistical Society. Series B (Methodological)*, 44–47.
- Strehler, B. L., & Mildvan, A. S. (1960). General Theory of Mortality and Aging. *Science*, 132(3418), 14–21.
- Tabeau, E., Van den Berg Jeths, A., & Heathcote, C. (2001). *Forecasting mortality in developed countries*. Springer.
- Thatcher, A., Kannisto, V., & Vaupel, J. (1998). *The force of mortality at ages 80 to 120* (Vol. 22). Odense University Press Odense.
- United Nations Population Division. (2015). *World Population Prospects: The 2015 Revision, Methodology of the United Nations Population Estimates and Projections* (No. Working Paper No. ESA/P/WP.242.).
- Vaupel, J. W., Carey, J. R., & Christensen, K. (2003). It's never too late. *Science*, 301(5640), 1679–1681.
- Vaupel, J., & Yashin, A. (1983). *The deviant dynamics of death in heterogeneous populations*. International Institute for Applied Systems Analysis.
- Vaupel, J., & Yashin, A. (1985). Heterogeneity's ruses: Some surprising effects of selection on population dynamics. *American statistician*, 176–185.
- Vaupel, J., Carey, J., Christensen, K., Johnson, T., Yashin, A., Holm, N., et al. (1998). Biodemographic trajectories of longevity. *Science*, 280(5365), 855.
- Vaupel, J., Manton, K., & Stallard, E. (1979). The impact of heterogeneity in individual frailty on the dynamics of mortality. *Demography*, 16(3), 439–454.
- Wang, J.-L., Muller, H.-G., & Capra, W. B. (1998). Analysis of Oldest-Old Mortality: Lifetables Revisited. *The Annals of Statistics*, 26(1), 126–163.
- Wasserman, L. (2013). *All of statistics: A concise course in statistical inference*. Springer Science & Business Media.
- Weibull, W. (1951). A Statistical Distribution Function of Wide Applicability. *Journal of applied mechanics*.
- Wickham, H. (2009). *Ggplot2: Elegant graphics for data analysis*. Springer New York.

- Wickham, H., Francois, R., Henry, L., & Müller, K. (2016). *Dplyr: A Grammar of Data Manipulation. R package version 0.5.0*. R Core Development Team Vienna.
- Wilmoth, J. R. (1995). Are mortality rates falling at extremely high ages? An investigation based on a model proposed by Coale and Kisker. *Population studies*, *49*(2), 281–295.
- Wrigley-Field, E. (2014). Mortality Deceleration and Mortality Selection: Three Unexpected Implications of a Simple Model. *Demography*, *51*(1), 51–71.
- Yashin, A. I., Iachine, I. A., & Begun, A. S. (2000). Mortality modeling: A review. *Mathematical Population Studies*, *8*(4), 305–332.
- Yashin, A., Vaupel, J., & Iachine, I. (1994). A duality in aging: The equivalence of mortality models based on radically different concepts. *Mechanisms of Ageing and Development*, *74*(1-2), 1–14.
- Yi, Z., & Vaupel, J. W. (2003). Oldest old mortality in China. *Demographic Research*, *8*, 215–244.

Online appendix

A Data

The Kannisto-Thatcher database contains data on deaths and exposure above age 80 for 35 countries, with some of the Scandinavian data going back to the mid-18th century (MPIDR 2014). However, data quality for mortality at advanced ages is a serious concern (Jdanov et al. 2008). In order to assess theories of old-age mortality by fitting hazard models to cohort data, we narrowed the Kannisto-Thatcher database down, focusing on cohorts for which very high-quality data mortality is available. We took several steps to select cohorts of very high quality. First, we use the analysis of Kannisto-Thatcher data quality reported in Jdanov et al. (2008) to identify countries for which over half of the available data years were of the highest quality, and the remaining years were of the second-highest quality. This set of countries that consistently produced high-quality data included Belgium, Czech Republic, Denmark, France, West Germany, Italy, Japan, the Netherlands, Poland, Scotland, Sweden, and Switzerland. From this subset of countries that produce high-quality data, we then chose the subset of years that Jdanov et al. (2008) assessed to have the highest quality.

Because we model deaths at ages 80 to 104, we also require information about deaths by single year of age in that age range. Many country-years in the Kannisto-Thatcher database have data reported by single year of age only up to age 99, 100, or 101; in these country years, an aggregate category is then used for older deaths. Importantly, the researchers who curate the Kannisto-Thatcher database assume a Kannisto model in order to assign deaths in the aggregate category to the individual ages (MPIDR 2014). Using cohorts whose data has been pre-processed using a Kannisto model would obviously confuse efforts to assess the fit of different mortality hazards to these data. Thus, we can only use country-years for which deaths are reported by single year of age up to 105⁹.

Putting these requirements together, Table 4 summarizes the cohorts for which high-quality data are available on deaths by single year of age for the entire time span that the cohort members were between the ages of 80 and 105. In total, there are 360 country-sex-cohorts of data from 10 different countries.

Table 4: Summary of the availability of high-quality data from the Kannisto-Thatcher database. Usable ages means that deaths are reported by single year of age up to at least age 105. The final dataset has data for 360 country-sex-cohorts.

Country	High quality years	Usable ages	Usable periods	Cohorts included
Belgium	1951-2000	1973+	1973-2000	1893-1895

⁹For a cohort born in year c , the first members will reach their 80th birthday in year $y_{\min} = c + 80$ and the last possible age at which cohort members could be 104 is $y_{\max} = c + 106$. Thus, to be able to model cohort c , I need high quality period data from the period $[c + 80, c + 106)$.

Country	High quality years	Usable ages	Usable periods	Cohorts included
Czech Republic	1951-1980	none	none	none
Denmark	1931-1950; 1961-2000	1943+	1943-1950; 1961-2000	1881-1895
France	1951-2000	1946- 1997;2002+	1946-1997	1866-1892
W. Germany	1971-2000	1964+	1971-2000	1891-1895
Italy	1961-2000	all	1961-2000	1881-1895
Japan	1971-2000	all	1971-2000	1891-1895
Netherlands	1951-2000	all	1951-2000	1871-1895
Poland	1971-2000	2002+	none	none
Scotland	1951-1960; 1971-1990	1963-2003	1971-1990	1891-1895
Sweden	1901-2000	all	1901-2000	1821-1895
Switzerland	1911-1920; 1931-1940; 1951-1960; 1971-2000	1950+	1951-1960; 1971-2000	1891-1895

B Methods

This appendix provides greater detail about the models and the methods used to fit each model to cohort death data. Appendix B.1 provides a more detailed explanation of the theory behind mortality hazards. Next, Appendix B.2 reviews the model that was introduced in the main text. Finally, Appendix B.3 provides some technical details related to fitting the hazard models by maximum likelihood.

B.1 Hazards and heterogeneity

Models of mortality at old ages can be expressed using hazard functions, which are mathematical descriptions of the risk of death by age. Researchers distinguish between the individual hazard function and the population hazard function. For a particular person, i , the *individual hazard function* is defined as

$$\mu_i(z) = -\frac{d \log S_i(z)}{dz} = -\frac{1}{S_i(z)} \frac{dS_i(z)}{dz}.$$

where $S_i(z)$ is the *individual survival function*, *i.e.* the probability that person i is alive at exact age z .

The individual hazard function is a useful theoretical concept, but it can never be empirically observed.¹⁰ Instead, researchers typically study deaths among groups of people. For a group of people, the *population hazard function* is defined as:

$$\mu(z) = -\frac{d \log S(z)}{dz} = -\frac{1}{S(z)} \frac{dS(z)}{dz}. \quad (7)$$

where $S(z)$ is the *population survival function*, *i.e.* the proportion of group members that survives to exact age z .

Mortality researchers are typically interested in individual-level hazards, but it is only possible to empirically estimate population-level hazards. What is the relationship between the individual and population hazard functions? If all of the people in a group face identical mortality hazards, then the population hazard function is the same as the group members' individual hazard function; intuitively, when all group members face identical mortality hazards, observing the group members' ages at death is equivalent to observing several lifetimes for one individual. On the other hand, if the people in a group face different individual hazards, then the population hazard function is not necessarily the same as any individual hazard; in fact, research on heterogeneity in mortality has shown that the population hazard can present a misleading picture of the underlying individuals' hazard functions (Vaupel and Yashin 1983, 1985; Vaupel et al. 1979; Wrigley-Field 2014; A. I. Yashin et al. 2000; A. Yashin et al. 1994). This stream of research has led to many different theories about how individual hazards might aggregate up into the population hazard. However, research on mortality heterogeneity has also led to the understanding that different combinations of individual hazard functions can lead to the same population hazard function (A. Yashin et al. 1994). Thus, studying the predictions made by population hazard functions about cohort deaths by age enables researchers to distinguish between some – but not all – theories about mortality; it is technically possible for different models to predict identical numbers of cohort deaths by age. When two different models predict exactly the same number of deaths by age, there is no way to distinguish between them without additional information. Thus, our design enables us to understand which *population hazards* best fit available data, but it does not enable us to distinguish between different theories that predict identical population hazards (Figure 1).

Given a model for the population hazard, there is a mathematical relationship that links the hazard function $\mu(z)$ and the probability of dying between ages z and $z + k$, conditional on surviving to age z :

¹⁰In order to obtain empirical information about the shape of a particular individual's mortality hazard function, it would be necessary to repeat the individual's life many times, recording the age at which the individual died each time. Of course, this is impossible.

$$\pi(z, z+k) = 1 - \exp\left(-\int_z^{z+k} \mu(x)dx\right). \quad (8)$$

Equation 10 shows that a population hazard function can be converted into expected numbers of cohort deaths by age. A theory that has been expressed as a hazard function can thus be tested by comparing predicted numbers of deaths by age to empirically observed numbers of deaths by age.

B.2 Model

In a population that faces identical hazards cohort deaths between ages z and $z+1$ are distributed binomially; that is, if N_z people from a cohort survive to exact age z , and all of the members of the cohort face the same hazard $\mu(z)$, then

$$D_z \sim \text{Binomial}(N_z, \pi(z, z+1)), \quad (9)$$

where D_z is the number of deaths between ages z and $z+1$, and $\pi(z, z+1)$ is the probability of dying between ages z and $z+1$. $\pi(z, z+1)$ is derived from the hazard function according to:

$$\pi(z, z+k) = 1 - \exp\left(-\int_z^{z+k} \mu(x)dx\right). \quad (10)$$

The likelihood for an observed sequence of deaths $\mathbf{D} = D_1, D_2, \dots$ and survivors to each age, $\mathbf{N} = N_1, N_2, \dots$ is then

$$Pr(\mathbf{D}|\mathbf{z}, \theta, \mathbf{N}) = \prod_z \binom{N_z}{D_z} \pi(z, \theta)^{D_z} (1 - \pi(z, \theta))^{(N_z - D_z)}.$$

Taking logs produces

$$l(\mathbf{D}|\mathbf{z}, \theta, \mathbf{N}) = K + \sum_z [D(z) \log(\pi(z, \theta)) + (N(z) - D(z)) \log(1 - \pi(z, \theta))], \quad (11)$$

where K is a constant that does not vary with θ . Finally, substituting in the relationship between the hazard function and the probability of death, we arrive at

$$\begin{aligned}
l(\mathbf{D}|\mathbf{z}, \mu, \theta) = K + \\
\sum_z \left[D(z) \log \left(1 - \exp \left(- \int_z^{z+k} \mu(x, \theta) dx \right) \right) + \right. \\
\left. (N(z) - D(z)) \exp \left(- \int_z^{z+k} \mu(x, \theta) dx \right) \right], \tag{12}
\end{aligned}$$

In order to fit each model to a cohort dataset, Equation 12 is maximized as a function of θ .

B.3 Estimation

In order to fit a model to a specific cohort dataset, we maximize the likelihood (Equation 11) numerically using the Broyden-Fletcher-Goldfarb-Shanno (BFGS) algorithm (Nocedal and Wright 1999). The BFGS algorithm is a numerical optimization routine that has been shown to work well for different settings and that is currently considered the most effective of the so-called quasi-Newton optimization routines (Nocedal and Wright 1999, pg. 139). Since the size of the problem we study here is not very large, we have no need to adopt limited memory BFGS, stochastic gradient descent, or other optimization routines that have become popular for problems with very large numbers of free parameters. BFGS has been implemented and widely used as part of the `optim` routine in the R statistical software package (R Core Team 2014). The exact parameterization used for each model is described in Appendix E.

In maximizing log-likelihoods, it is common to omit constant factors that do not vary with model parameters. In general, in order to calculate AIC and BIC values that compare different probability models, it is important to retain these constant factors. In this study, the probability model is the same for all of the models—*i.e.*, given conditional probabilities of death, the deaths are distributed binomially. Thus, in calculating Δ AIC and Δ BIC, these constants cancel out.

We took several steps to ensure that the BFGS optimization routine behaved well. First, for each model, we derived closed-form expressions¹¹ for (1) the exponentiated integral that converts hazards to probabilities (Equation 2)¹²; (2) the partial derivative of the likelihood with respect to each parameter value (*i.e.*, partial derivatives of Equation 11 with respect to each entry of the vector θ). Several of the mathematical expressions that result are complex and unwieldy; thus, to minimize the risk of errors in translating the mathematical expressions into computer code, we used the

¹¹The hazard to probability integral for the log-quadratic model involves the error function (Abramowitz and Stegun 1964; Stein 2008); thus, this result is technically not in closed form. However, the error function has been widely studied and highly accurate approximations are available.

¹²Many previous studies have used approximations to convert the hazard into conditional probabilities of death, particularly in the context of regression approaches to fitting mortality models. Wang et al. (1998) points out that these approximations can be problematic, particularly at oldest ages. Thus, an additional advantage to deriving analytical expressions for the conditional probability of death is that it avoids the need to make such approximations.

Sage symbolic computing package to programmatically generate C++ code needed to calculate each analytical expression (Stein 2008). All of the generated code can be seen in the open-source `mortfit` package, and the analytic expression for converting hazards into conditional probabilities of death are shown in Appendix E.

Second, in order to guard against the possibility that the BFGS algorithm converges prematurely or to a local optimum, we maximize the likelihood many different times (11 in total). The first time we maximize the likelihood, we use a heuristic to crudely estimate initial parameter values. The heuristic used is different for each model and a detailed explanation of each heuristic is described along with the individual hazard functions in Appendix E. For each of the remaining 10 times the BFGS routine is used to maximize the likelihood, we choose random starting values for the parameters. The support of the random starting values was determined from initial runs of the model fits; these initial runs and experiments also guide the parameter scaling. After estimating θ for eleven different sets of starting values, we pick the result that has the highest value of the log-likelihood.

Finally, as we developed the routines used to fit the models, we also added the capability to examine likelihood profile plots and to fit models using grid searches to the `mortfit` package. We found likelihood profile plots to be helpful in initial development of the optimization strategy, but we did not find that grid search added value above and beyond using many random starts. Further, grid search can demand intensive computing resources; thus, we did not use grid search for the final results.

C Additional empirical results

This Appendix provides additional empirical results based on alternative, principled approaches to assessing model fit. We review two additional approaches to model selection: Section C.1 discusses the BIC; and Section C.2 discusses K -fold cross validation. The goal of this study is not to argue that one of these methods is definitively more appropriate than the others; all three of these approaches have been the subject of theoretical and empirical motivation, and each has merits and limitations.

C.1 Bayesian Information Criterion (BIC)

The BIC can be written as

$$\text{BIC} = -2\mathcal{L} + \log(n)k, \tag{13}$$

where \mathfrak{L} is the value of the maximized log-likelihood, k is the number of parameters (*i.e.*, the dimension of θ), and n is the size of the cohort. As was the case with the AIC, the BIC looks relatively simple, but it is justified by rigorous theory. Intuitively, the BIC is similar to the AIC, except that the BIC multiplies the number of parameters in the model by $\log(n)$ instead of 2. Since $\log(n) > 2$ as long as n is at least 8, this means that the BIC penalizes complex models more heavily than the AIC.

The theory that motivates the BIC usually posits a Bayesian setup with weak priors on the model parameter values and uniform priors over the candidate models. If the true, data-generating model is in the candidate set, one can show that the BIC is then consistent in the sense that the BIC will tend to select the true data-generating model with probability 1 as the sample size n goes to infinity. However, it seems unrealistic to think that the true data-generating model will ever really be in the candidate set; the more relevant question seems to be: which of the candidate models makes the most accurate empirical predictions? Viewed from that perspective, the BIC is a model selection criterion that more heavily penalizes complex models than the AIC; indeed, some evidence suggest that the BIC can favor overly simple models (Burnham and Anderson 2004; Claeskens and Hjort 2008, Ch. 4; Efron and Hastie 2016, Ch. 13).

Like the AIC, absolute BIC values are not comparable across datasets, but relative values are. Thus, following Burnham and Anderson (2004), we use the quantity ΔBIC , defined in the same way as ΔAIC , to compare model fits across all cohorts in our sample.

More detailed discussions of the BIC, including comparisons with the AIC, can be found in Claeskens and Hjort (2008); Burnham and Anderson (2003); Burnham and Anderson (2004); Hoeting et al. (1999); Friedman et al. (2009); and Kass and Raftery (1995).

Results using the BIC

In this section, we present summaries of model fits across the 360 cohorts as evaluated by the BIC. In general, the BIC can be expected to prefer models with fewer parameters than those selected by the AIC; in the results here, this preference for less complex models is most evident in the comparatively better performance of the two-parameter Kannisto and Gompertz models.

Appendix Figure 7 shows boxplots that summarize the ΔBIC values by model across all 360 cohorts; this figure is analogous to Figure 3. According the ΔBIC , the two-parameter Kannisto model performs the best.

Appendix Figure 8 shows ΔBIC results analogous to the ΔAIC results presented in Figure 4. Appendix Figure 8 compares the fraction of cohorts for which each model enjoys substantial support from the data ($\Delta\text{BIC} \leq 2$) to the fraction of cohorts for which each model has almost no support

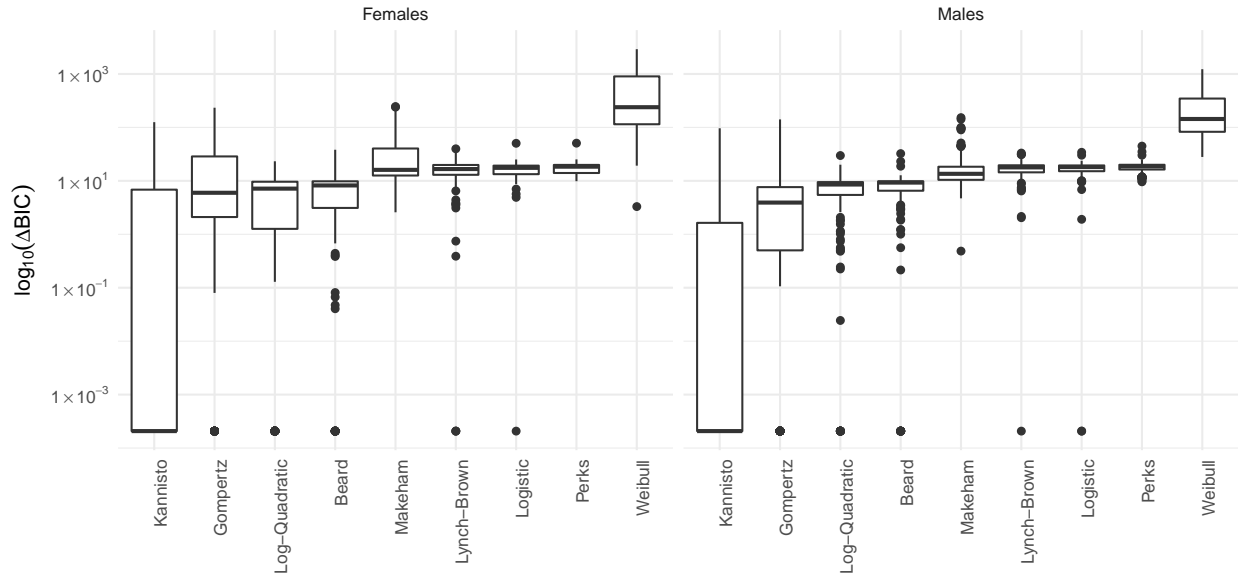


Figure 7: Boxplots summarizing the distributions of ΔBIC across all of the cohorts in the sample (note that the y axis is on a log scale). The horizontal line shows the median, the edges of the box show the interquartile range, and the whiskers extend to the largest and smallest values within 1.5 times the interquartile range; more extreme points are plotted separately. The Kannisto model appears to perform the best.

from the data ($\Delta\text{BIC} > 10$). The figure dramatically separates models according to the number of parameters they have. The Kannisto model is the best performer, with substantial support from the data ($\Delta\text{BIC} \leq 2$) in about three quarters of the cohorts, and essentially no support from the data ($\Delta\text{BIC} > 10$) in fewer than one quarter of the cohorts. The Gompertz model (2 parameters) and the Log-Quadratic and Beard models (3 parameters) are in the lower-left corner of the plot: these models infrequently have substantial support from the data ($\Delta\text{BIC} \leq 2$), but they also infrequently have essentially no support from the data ($\Delta\text{BIC} > 10$). All of the remaining models are in the top-left corner of the plot, meaning that ΔBIC suggests that they have little empirical support.

Appendix Figure 9 shows ΔBIC results analogous to the ΔAIC results presented in Figure 6. Appendix Figure 9 breaks the results in Appendix Figure 8 down by country for the five countries in the sample that have more than 10 cohorts worth of data. The figure shows that for Denmark, the Netherlands, and Sweden, the Kannisto model performs well. For Italy, and for French females, the Log-Quadratic model is preferred. More generally, consistent with the findings from Appendix Figure 8, results using ΔBIC heavily penalize more complex models: models with four parameters (Logistic and Lynch-Brown) never perform well.

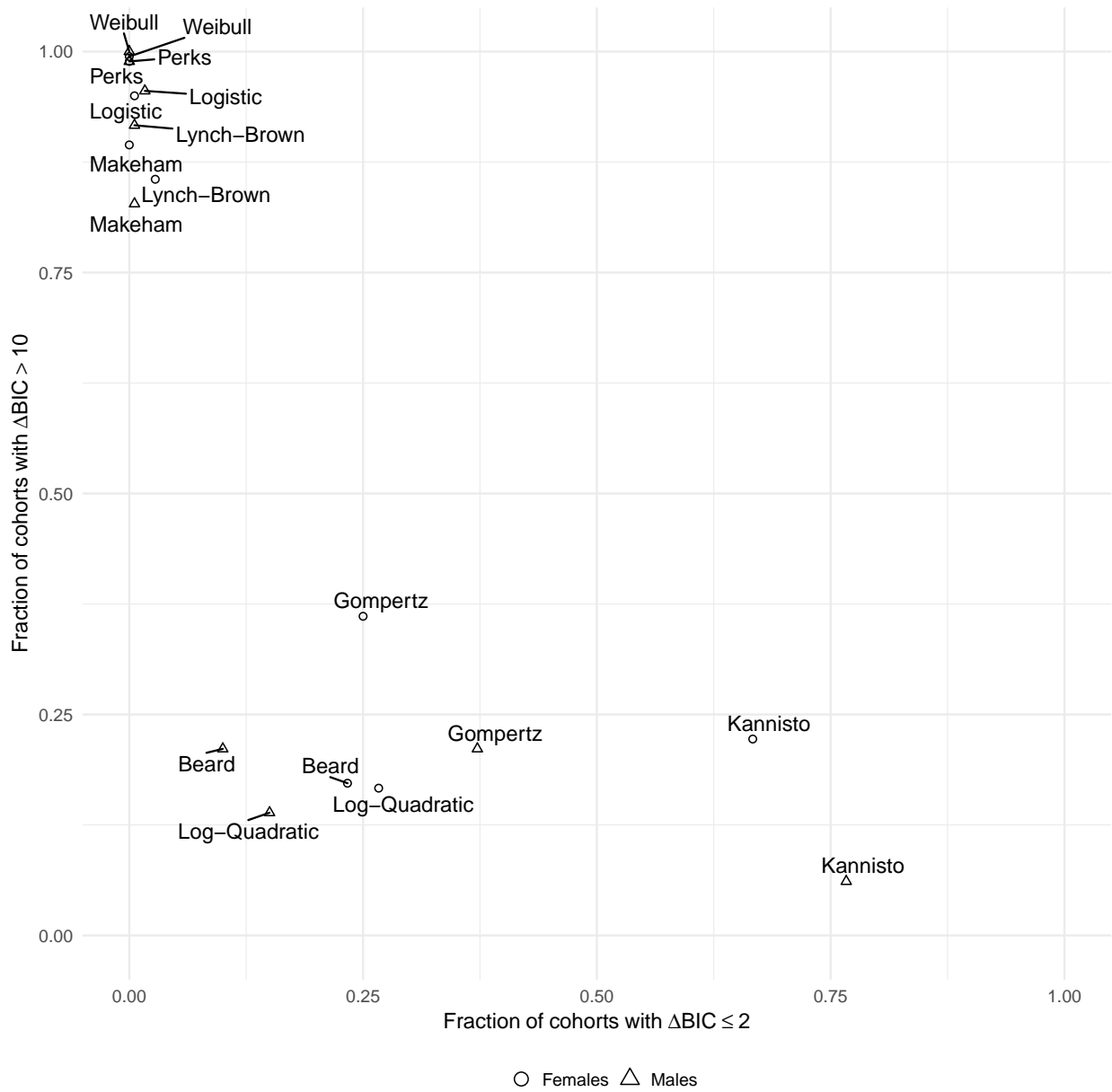


Figure 8: Fraction of cohorts for which the fit of each model had substantial support ($\Delta\text{BIC} \leq 2$, x axis) compared to the fraction of cohorts for which the fit of each model had essentially no support ($\Delta\text{BIC} > 10$, y axis). Models in the lower-right corner consistently fit the cohorts in the sample well; models in the lower-left corner are neither very good nor very bad; models in the upper-left corner consistently fit the cohorts in the sample poorly.

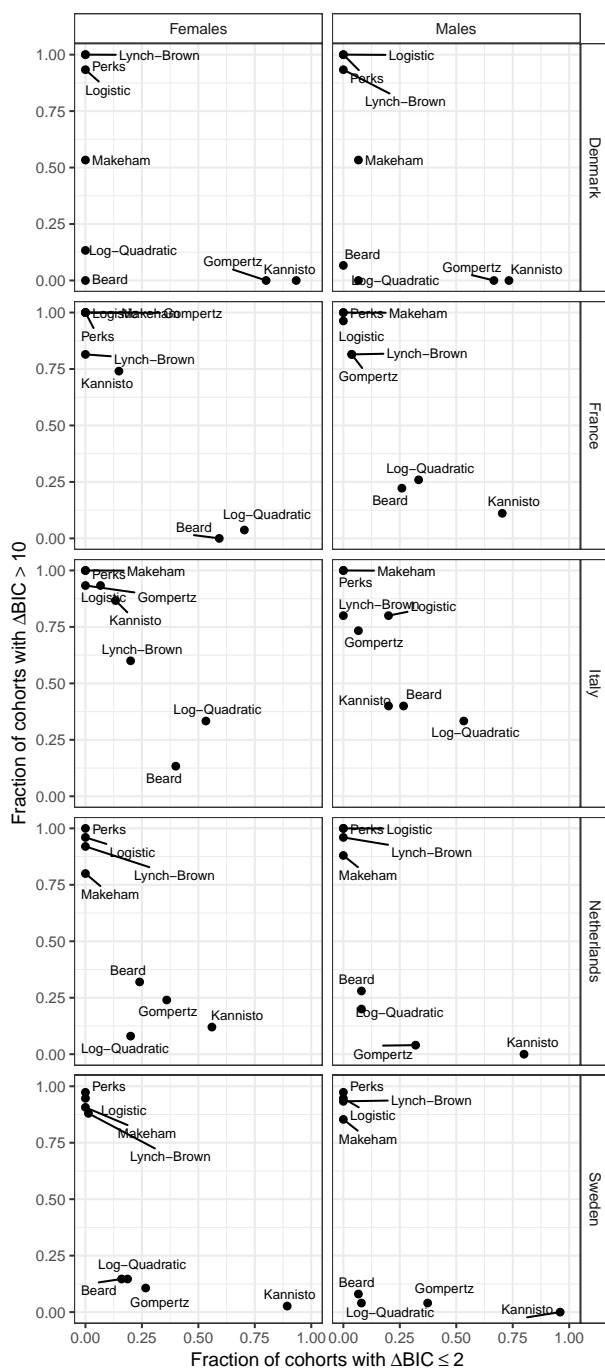


Figure 9: Fraction of cohorts for which the fit of each model had substantial support ($\Delta BIC \leq 2$, x axis) compared to the fraction of cohorts for which the fit of each model had essentially no support ($\Delta BIC > 10$, y axis) for each sex and for each country with at least ten cohorts of data. Models in the lower-right corner consistently fit the cohorts in the sample well; models in the lower-left corner are neither very good nor very bad; models in the upper-left corner consistently fit the cohorts in the sample poorly.

C.2 K -fold cross validation

K -fold cross validation is based on the idea that a dataset can be randomly split into K different parts, called *folds*. The model being studied can then be fit to $K-1$ of the folds (the *training set*), and the fitted model can be used to predict the outcome—*i.e.*, the number of deaths by age—for the remaining fold (the *test set*). Intuitively, this process overcomes the problem of overfitting because the parameters are estimated from one part of the data, and then the accuracy is assessed on a different part of the data. Thus, if stochastic noise from the training set had a large influence on parameter estimates, that will lead to error when the fitted model is used to predict deaths in the test set. In K -fold cross validation, this process can be repeated K times, each time picking a different fold to serve as the hold-out sample. Overall measures of prediction error can then be averaged over the K different cross-validation error estimates. Friedman et al. (2009), Wasserman (2013), and Efron and Hastie (2016) have introductions to K -fold cross validation.

Cross validation has been the subject of somewhat less theoretical analysis than AIC and BIC, but it is appealing because it can be easily used for a wide range of different models, including nonparametric models and prediction algorithms that are not even based on probability distributions. Cross validation has become increasingly popular as computation has become relatively cheap and because it has been very influential in machine learning. To the extent that cross validation has been theoretically studied, its motivation is similar to the AIC; for example, leave-one-out cross validation has been shown to be asymptotically equivalent to the AIC (Burnham and Anderson 2003; Claeskens and Hjort 2008; Stone 1977). More generally, the AIC and cross validation both aim to reflect a model’s predictive ability. Cross validation is extremely flexible, while the AIC is more efficient in the sense that it provides less noisy measures of predictive ability (Efron and Hastie 2016, Ch. 12).

For cohort death data, the number of observations is given by the size of the cohort at the start of the youngest age group. The `mortfit` package has functions that can be used to split cohort death datasets into K folds, and the model estimation routines described in Appendix B.3 can be repeated for each fold. For example, within each fold, the model is fit with 11 different starting values, one based on heuristics and ten picked randomly. The results are used to estimate prediction error. The results here use $K = 5$ folds.

Results using K -fold cross-validation

In this section, we present summaries of model fits across the 360 cohorts as evaluated by 5-fold cross validation. In general, theoretical results show that cross validation can be expected to prefer similar models to the AIC, though the AIC is more efficient (Appendix C.2).

For K -fold cross validation, there is no direct analog to ΔAIC . Thus, we present results based on the rank of each model within each cohort. Since the Weibull model consistently performs very poorly, we omit it from these summaries. Thus, within each cohort, model ranks range from 1 (best fit) to 8 (worst fit).

Appendix Figure 10 shows the distribution of ranks across the 360 cohort fits for each model, and for each sex. According to the median rank, the top-performing models are the Lynch-Brown, Logistic, Beard, and Log-Quadratic; the bottom performers are the Gompertz and Makeham models. As would be expected from statistical theory, the results in Appendix Figure 10 suggest that K -fold cross validation penalizes complex models less heavily than the BIC, and more similarly to the AIC.

Appendix Figure 11 compares the fraction for cohorts for which each model is in the top 2 (x axis) to the fraction of cohorts for which each model is in the bottom two (y axis). The figure shows that, according to 5-fold cross validation, the Makeham and Gompertz models consistently perform more poorly than all of the others. The remaining models are remarkably similar to one another in terms of their performance; the point estimates in Appendix Figure 11 suggest that the Lynch-Brown and Log-Quadratic models attain a good trade-off between consistently fitting relatively well and rarely fitting relatively poorly.

Finally, Appendix Figure 12 breaks the 5-fold cross validation results down by country, for the five countries that have data for more than 10 cohorts per sex. This figure is similar in spirit to Figure 6, but it is based on a different metric and thus not directly comparable. The figure shows that 5-fold cross validation results differ by country, but differences using this summary plot are less salient than they were using ΔAIC . The most distinctive feature of France and Italy is that they both show the Makeham and Gompertz model consistently performing poorly, relative to the other models.

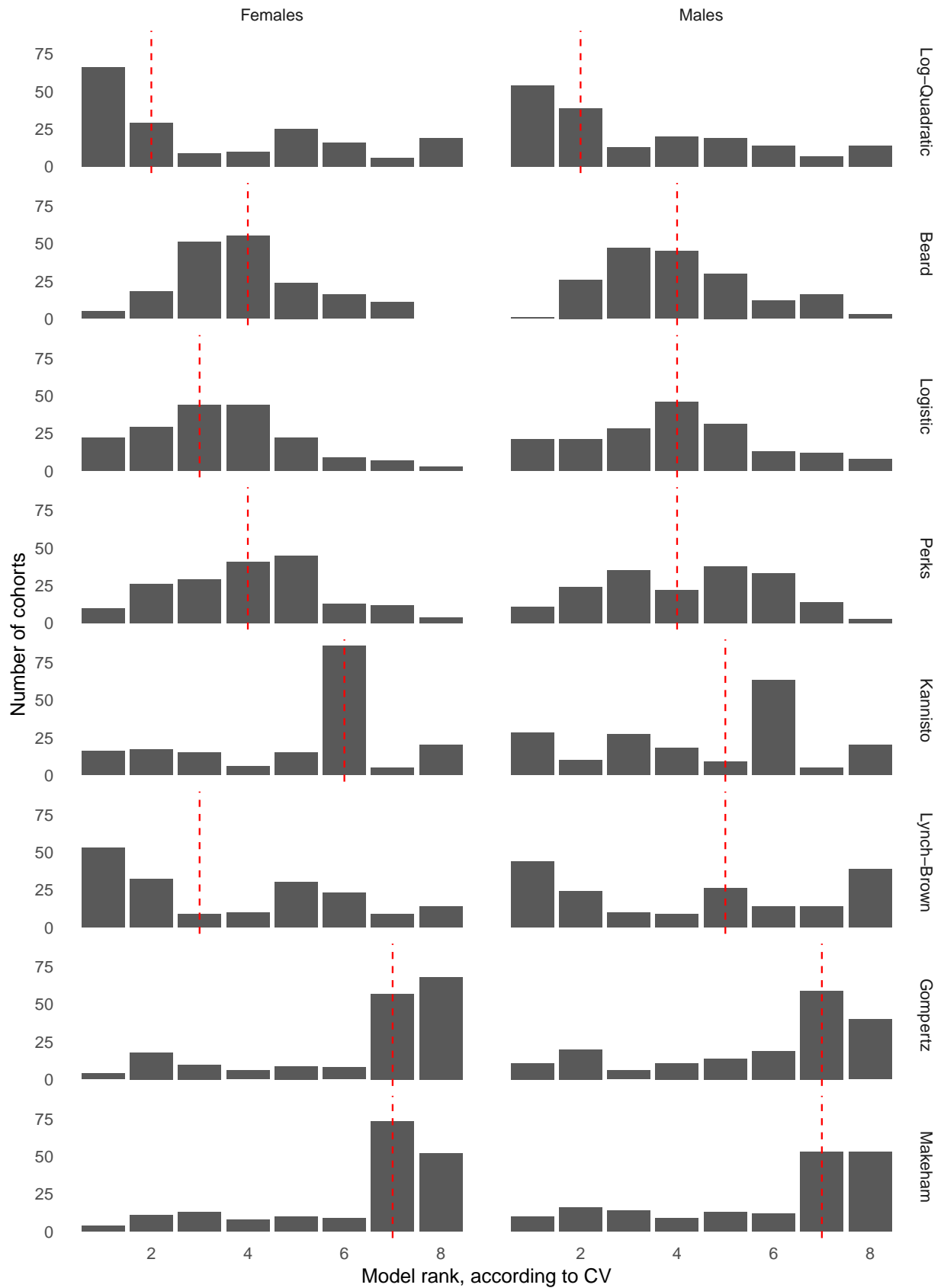


Figure 10: Distribution of model rank by 5-fold cross-validation, with 1 being the best prediction and 8 being the worst. Male cohorts are in the left column and female cohorts are in the right column. The dashed vertical lines show the median rank for each model.

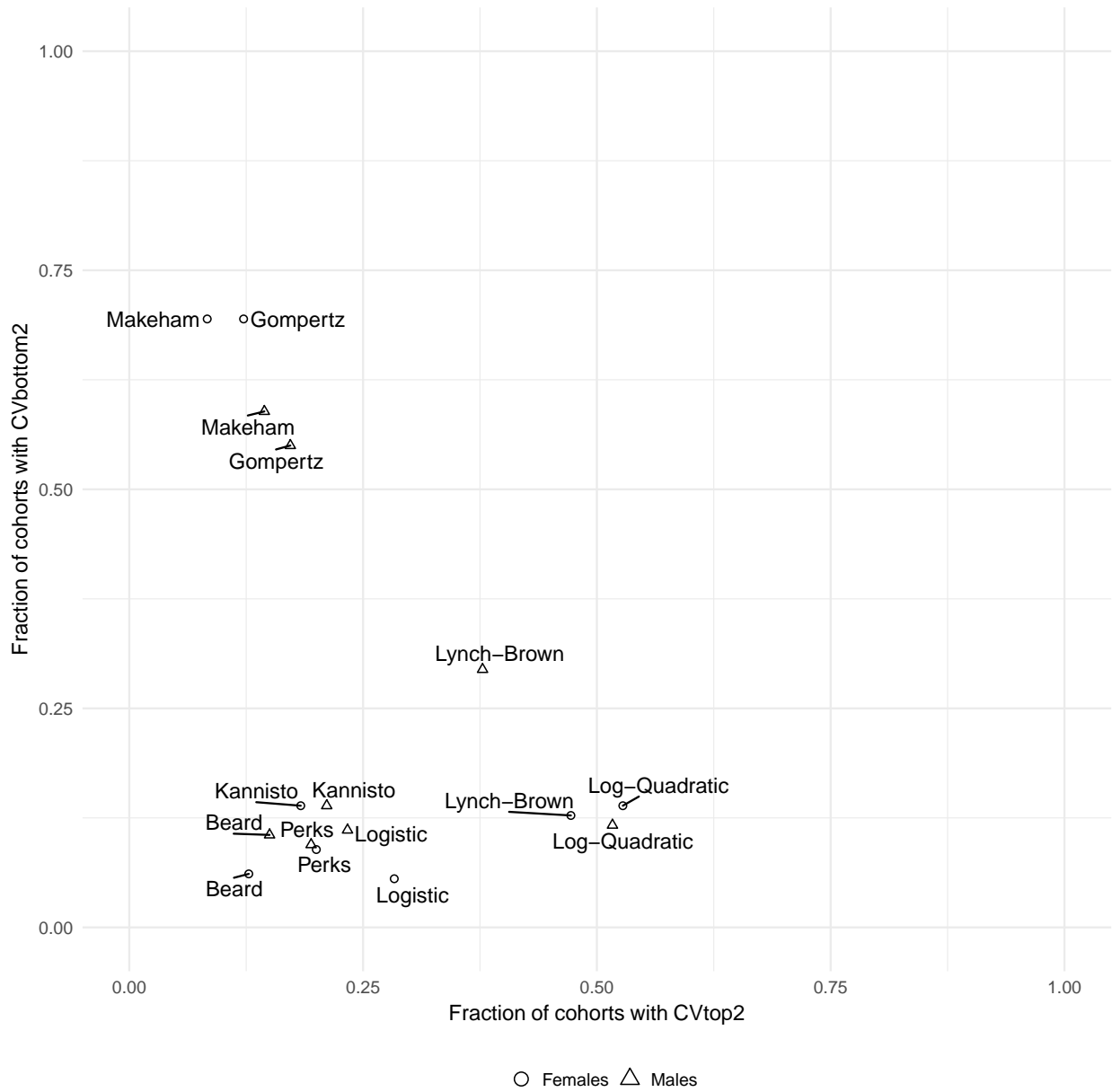


Figure 11: Fraction of cohorts for which the cross-validation error of each model was very good (best or second-best, x axis) and very poor (worst or second-worst, y axis). Models in the lower-right corner consistently produced low cross-validation error; models in the lower-left corner had neither consistently low cross-validation error nor consistently high cross-validation error; models in the upper-left corner had consistently high cross-validation error.

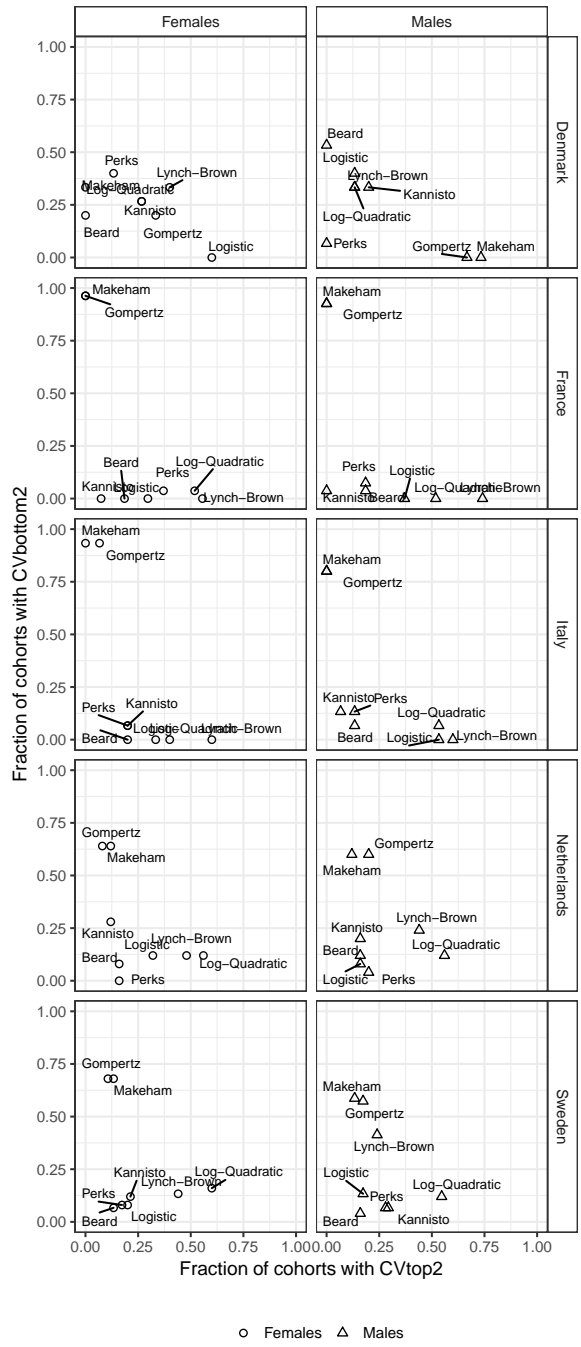


Figure 12: Fraction of cohorts for which the cross-validation error of each model was very good (best or second-best, x axis) and very poor (worst or second-worst, y axis) by country. Models in the lower-right corner consistently produced low cross-validation error; models in the lower-left corner had neither consistently low cross-validation error nor consistently high cross-validation error; models in the upper-left corner had consistently high cross-validation error.

D Illustrative simulation: sample size

We found that patterns of model fit varied by country, and that this variation was related to how poorly the Gompertz/Makeham models fit cohorts from each country. At one extreme, the Gompertz/Makeham models did not fit France and Italy well at all; at the other extreme, the Gompertz/Makeham models did not produce poor predictions for Denmark (though they were not the best performers). One possible explanation for this difference is sample size: cohorts from Italy and France are roughly 5 to 10 times larger than cohorts from Sweden, Denmark, and the Netherlands (Table 2). Thus, in a small country like Denmark, it may be the case that small sample sizes do not provide enough information to reliably detect non-Gompertz patterns in old-age death rates, even if the underlying mortality process is non-Gompertzian.

Although we cannot examine how model fits would be affected if we observed bigger cohorts from Denmark, we can examine how our inferences about bigger countries would be affected if we observed smaller cohorts. To investigate this question, we started with the cohort of French Females born in 1872 and successively reduced the cohort size. At each reduced size, we re-fit all of the models and calculated ΔAIC . Figure 13 shows that, as expected, reducing the size of the cohorts led simpler, two parameter models to perform relatively better. However, the Gompertz model never emerges as the best; instead, in the regime where two-parameter models are favored (below about 30% of the original cohort size), the Kannisto model – which has a sigmoid shape, allowing for decelerating death rates – is the one that emerges as the best. This suggests that, at least for France, if cohorts had been smaller but generated by the same underlying mortality dynamics, we may have found that the Kannisto model was most accurate, but we would not have selected the Gompertz model.

French Females 1872

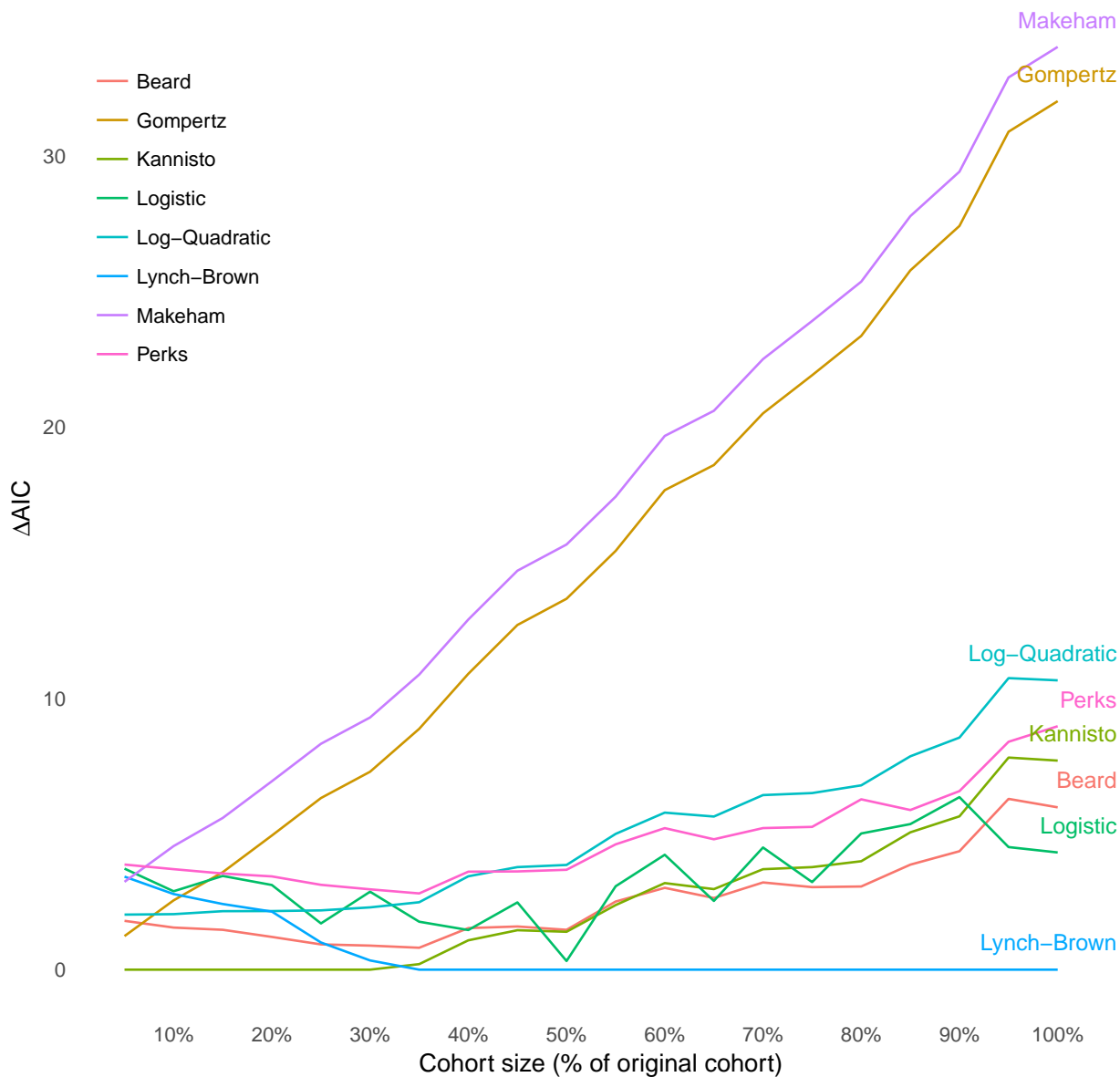


Figure 13: Simulation showing the effect of reducing cohort size on ΔAIC using data from French Females in 1872. The Lynch-Brown model fits the original cohort best. However, as the size of the cohort is reduced, simpler models perform better; at around 30% of the original sample size, the two-parameter Kannisto model is estimated to fit better than the four-parameter Lynch-Brown model. The Gompertz model improves with reduced sample size, but it never surpasses the sigmoid-shaped Kannisto model.

E Models

This appendix contains detailed information about each model, including some references to the literature and details about how the model was parameterized and fit.

E.1 Gompertz

The Gompertz function is one of the oldest and most common parametric description of death rates in demography. It was first introduced in Gompertz (1825) and its simplicity and interpretability have meant that it continues to be used today (S. Preston et al. 2000).

Hazard function

The Gompertz hazard can be written

$$\mu(z) = \alpha \exp(\beta z),$$

where $\alpha > 0$.

E.1.1 Parameters

The parameterization used in the `mortfit` package is given in Table 5.

model	code
$\alpha \in (0, \infty)$	$\exp(\theta_1)$
$\beta \in (-\infty, \infty)$	θ_2

Table 5: The parameterization of the Gompertz hazard used in the `mortfit` package.

Starting values

In order to choose the starting values for the BFGS optimization algorithm, we estimate a regression of the log central death rates on age; that is, we fit

$$\log(M_z) = \alpha_0 + \beta_0 z + \epsilon. \tag{14}$$

We then use the preliminary estimates of α_0 and β_0 as our starting values.

Conditional probability of death

$${}_1q_z = 1 - \exp\left(-\int_z^{z+1} \mu(x)dx\right) = 1 - \exp\left(-\frac{\alpha}{\beta}\left(e^{\beta(z+1)} - e^{\beta z}\right)\right) \quad (15)$$

E.2 Makeham

Makeham (1860) proposed adding an additional parameter to the Gompertz function; this additional parameter is often interpreted as a baseline level of extrinsic mortality.

Hazard function

The Makeham hazard function can be written

$$\mu(z) = \gamma + \alpha \exp(\beta z). \quad (16)$$

Parameters

model	code
$\alpha \in (0, \infty)$	<code>exp(θ_1)</code>
$\beta \in (-\infty, \infty)$	<code>θ_2</code>
$\gamma \in (0, \infty)$	<code>exp(θ_3)</code>

Table 6: The parameterization of the Makeham hazard used in the `mortfit` package.

Starting values

In order to choose starting values for the BFGS algorithm, we follow a procedure similar to the one we used for the Gompertz model. First, we choose $\gamma_0 = \exp(\zeta)$, where ζ is a very small value. Next, we estimate a regression of the log central death rates on age; that is, we fit

$$\log(M_z - \gamma_0) = b_0 + b_1 z + \epsilon. \quad (17)$$

For the starting parameter estimates we use $\alpha_0 = \exp(b_0)$ and $\beta_0 = b_1$.

Conditional probability of death

$${}_1q_z = 1 - \exp\left(-\int_z^{z+1} \mu(x) dx\right) = 1 - \exp\left(-\frac{\alpha(e^{\beta(z+1)} - e^{\beta z})}{\beta} - \gamma\right) \quad (18)$$

E.3 Logistic

We follow A. Thatcher et al. (1998) in calling this the logistic hazard, though several other hazard functions have logistic shapes. The study of logistic-shaped hazard functions, including (but not limited to) this one has a long history; starting with Perks (1932), and including many subsequent studies (R. E Beard 1959, L. A Gavrilov and Gavrilova (1991), A. Yashin et al. (1994), Le Bras (1976), Vaupel et al. (1979)).

Note that when $\delta = 0$, this particular logistic form simplifies to be Makeham.

Hazard function

The Perks-Beard logistic hazard is given by

$$\mu(z) = \gamma + \frac{\alpha \exp(\beta z)}{1 + \delta \exp(\beta z)}, \quad (19)$$

where $\alpha > 0$, $\beta > 0$, $\gamma > 0$, and $\delta > 0$.

Parameters

model	code
$\alpha \in (0, \infty)$	$\exp(\theta_1)$
$\beta \in (0, \infty)$	$\exp(\theta_2)$
$\gamma \in (0, \infty)$	$\exp(\theta_3)$
$\delta \in (0, \infty)$	$\exp(\theta_4)$

Table 7: The parameterization of the Logistic hazard used in the `mortfit` package.

A. Thatcher et al. (1998) reparameterized this using

$$\alpha = \frac{ba}{b - \sigma^2 a} \quad (20)$$

$$\beta = b \quad (21)$$

$$\gamma = c \quad (22)$$

$$\delta = \frac{b}{\sigma^2 a} - 1 \quad (23)$$

to yield the expression

$$\mu(z|a, b, c, d) = c + \frac{a \exp(bz)}{1 + \sigma^2 \frac{a}{b} (\exp(bz) - 1)}. \quad (24)$$

This is useful in studies of heterogeneity; however, in this analysis we employ the original parameterization.

Starting values

Choosing starting values for the BFGS optimization algorithm is somewhat tricky. First, we summarize a few derivations that are used in our approach. Analytically, the inflection point in the logsitic curve—the point at which the second derivative with respect to age is equal to 0—will be attained when

$$z_{\text{inf}} = -\frac{\log(\delta)}{\beta}. \quad (25)$$

Furthermore, the slope at the inflection point will be

$$\left. \frac{d\mu(z)}{dz} \right|_{z=z_{\text{inf}}} = \mu'(z_{\text{inf}}) = \frac{\alpha\beta}{4\delta}.$$

This means that we have

$$\beta = \frac{4\delta\mu'(z_{\text{inf}})}{\alpha}. \quad (26)$$

In order to choose starting values for the optimization routine, we start by using the observed central death rates M_z as preliminary estimates. We fit a logistic regression of the observed central death rates on age, with each age weighted by the amount of exposure we observe. Following a procedure similar to the one described for the Lynch-Brown form, we use the fitted values from the model to estimate the age at which the median of the range of observed central death rates is attained; this is z_{inf} , our crude estimate of the inflection point in the central death rates.

Now note that

$$\lim_{z \rightarrow \infty} \mu(z) = \frac{\alpha}{\delta} + \gamma. \quad (27)$$

Since we expect γ to be small, $\lim_{z \rightarrow \infty} \mu(z) \approx \frac{\alpha}{\delta}$. Therefore, for our starting point β_0 , we combine Equation 26 and Equation 27 to make the crude estimate $\beta_0 = 4 \mu'(z_{\text{inf}})/M_{\text{max}}$, where M_{max} is the maximum of the observed central death rates. Then, using Equation 25, we set the starting point for δ to be $\delta_0 = \exp(-\beta/z_{\text{inf}})$.

Next, again taking advantage of the fact that γ is typically very small, and using Equation 27, we set the starting point for α to be $\alpha_0 = \delta_0 M_{\max}$.

Finally, note that

$$\lim_{z \rightarrow 0} \mu(z) = \gamma + \frac{\alpha}{1 + \delta}. \quad (28)$$

We use this limit to choose a starting point for γ : $\gamma_0 = M_{\min} - \frac{\alpha_0}{1 + \delta_0}$, where M_{\min} is the smallest observed central death rate in the youngest age groups.

Like the starting points we use for all of the functional forms, the main goal here is to be sure the optimization routine starts with very approximately reasonable parameter values.

Conditional probability of death

$${}_1q_z = 1 - \exp\left(-\int_z^{z+1} \mu(x) dx\right) \quad (29)$$

$$= 1 - \exp\left(-\frac{\alpha \left[\log(\beta \delta e^{\beta(z+1)} + \beta) - \log(\beta \delta e^{\beta z} + \beta)\right]}{\beta \delta} - \gamma\right) \quad (30)$$

$$= 1 - \exp(-\gamma) \exp\left(-\frac{\alpha \left[\log(\beta \delta e^{\beta(z+1)} + \beta) - \log(\beta \delta e^{\beta z} + \beta)\right]}{\beta \delta}\right) \quad (31)$$

$$= 1 - \exp(-\gamma) \exp\left(\log(\beta \delta e^{\beta(z+1)} + \beta) - \log(\beta \delta e^{\beta z} + \beta)\right)^{-\frac{\alpha}{\beta \delta}} \quad (32)$$

$$= 1 - \exp(-\gamma) \left(\frac{\beta \delta e^{\beta(z+1)} + \beta}{\beta \delta e^{\beta z} + \beta}\right)^{-\frac{\alpha}{\beta \delta}} \quad (33)$$

$$= 1 - \exp(-\gamma) \left(\frac{\delta e^{\beta(z+1)} + 1}{\delta e^{\beta z} + 1}\right)^{-\frac{\alpha}{\beta \delta}} \quad (34)$$

$$= 1 - \exp(-\gamma) \left(\frac{\delta e^{\beta z} + 1}{\delta e^{\beta(z+1)} + 1}\right)^{\frac{\alpha}{\beta \delta}}. \quad (35)$$

E.4 Kannisto

The Kannisto model is a special case of the Logistic hazard where $\alpha = \delta$. A. Thatcher et al. (1998) trace its origins to a presentation given by Kannisto in 1992, and also to Himes et al. (1994). A. Thatcher et al. (1998) concluded that the Kannisto model, along with the Logistic model, was the best of the set they tested.

Hazard function

The Kannisto hazard can be written

$$\mu(z) = \frac{\alpha \exp(\beta z)}{1 + \alpha \exp(\beta z)}, \quad (36)$$

where $\alpha > 0$ and $\beta > 0$.

Parameters

model	code
$\alpha \in (0, \infty)$	$\exp(\theta_1)$
$\beta \in (0, \infty)$	$\exp(\theta_2)$

Table 8: The parameterization of the Kannisto hazard used in the `mortfit` package.

Starting values

In order to choose the starting values for the BFGS optimization algorithm, we estimate a logistic regression of the central death rates on age; that is, we use R's `glm` function to fit:

$$\text{logit}^{-1}(M_z) = a + bz. \quad (37)$$

We then use the coefficient estimates from the regression for starting values: for α , we use $\alpha_0 = \exp(a)$ (equivalently, because of our parameterization, θ_1 starts at a); and for β , we use $\beta_0 = b$ (equivalently, because of our parameterization, θ_2 starts at $\log b$).

Conditional probability of death

$${}_1q_z = 1 - \exp\left(-\int_z^{z+1} \mu(x)dx\right) \quad (38)$$

$$= 1 - \exp\left(-\frac{\log(\alpha\beta e^{\beta(z+1)} + \beta) - \log(\alpha\beta e^{\beta z} + \beta)}{\beta}\right) \quad (39)$$

$$= 1 - \exp\left(\left[\log(\alpha\beta e^{\beta z} + \beta) - \log(\alpha\beta e^{\beta(z+1)} + \beta)\right]^{1/\beta}\right) \quad (40)$$

$$= 1 - \exp\left(\log\left(\frac{\alpha\beta e^{\beta z} + \beta}{\alpha\beta e^{\beta(z+1)} + \beta}\right)^{1/\beta}\right) \quad (41)$$

$$= 1 - \left(\frac{\alpha e^{\beta z} + 1}{\alpha e^{\beta(z+1)} + 1}\right)^{1/\beta} \quad (42)$$

$$(43)$$

E.5 Beard / Gamma-Gompertz

The Beard model is a type of logistic hazard that can be derived from a model in which (1) individuals share a common baseline hazard and (2) each individual has a fixed frailty parameter which is multiplied by the baseline hazard to produce the individual hazard; and (3) these individual fixed frailty parameters have a Gamma distribution. This model has been widely studied; see, for example, R. E Beard (1959), K. G. Manton et al. (1981), and Horiuchi and Wilmoth (1998).

E.5.1 Hazard function

The Beard hazard has the form

$$\mu(z) = \frac{\alpha \exp(\beta z)}{1 + \delta \exp(\beta z)}, \quad (44)$$

where $\alpha > 0$, $\beta > 0$, and $\delta > 0$.

E.5.2 Parameters

model	code
$\alpha \in (0, \infty)$	$\exp(\theta_1)$
$\beta \in (0, \infty)$	$\exp(\theta_2)$
$\delta \in (0, \infty)$	$\exp(\theta_3)$

Table 9: The parameterization of the Beard hazard used in the `mortfit` package.

E.5.3 Starting values

We adopt the same approach used for the logistic function, except that we do not need starting values for γ , since that parameter is not in the Beard hazard.

E.5.4 Conditional probability of death

The conditional probability of death for the Beard hazard is the same as for the logistic hazard with γ fixed at 0. Thus,

$${}_1q_z = 1 - \exp\left(-\int_z^{z+1} \mu(x)dx\right) \quad (45)$$

$$= 1 - \left(\frac{\delta e^{\beta z} + 1}{\delta e^{\beta(z+1)} + 1}\right)^{\frac{\alpha}{\beta\delta}}. \quad (46)$$

E.6 Perks / Gamma-Makeham

The Perks model is another type of logistic hazard. While the Beard population hazard can be derived from a model that assumes a Gamma-Gompertz distribution of individual hazards, the Perks model can be derived from a model that assumes a Gamma-Makeham distribution of individual hazards. See, for example, K. G. Manton et al. (1981), and Horiuchi and Wilmoth (1998).

E.6.1 Hazard function

The Perks hazard has the form

$$\mu(z) = \frac{\gamma + \alpha \exp(\beta z)}{1 + \delta \exp(\beta z)}, \quad (47)$$

where $\alpha > 0$, $\beta > 0$, $\gamma > 0$, and $\delta > 0$.

E.6.2 Parameters

model	code
$\alpha \in (0, \infty)$	$\exp(\theta_1)$
$\beta \in (0, \infty)$	$\exp(\theta_2)$
$\gamma \in (0, \infty)$	$\exp(\theta_3)$
$\delta \in (0, \infty)$	$\exp(\theta_4)$

Table 10: The parameterization of the Perks hazard used in the `mortfit` package.

E.6.3 Starting values

We use the same approach described for the Logistic function to choose starting values when fitting the Perks hazard.

E.6.4 Conditional probability of death

The conditional probability of death for the Perks hazard is

$${}_1q_z = 1 - \exp\left(-\int_z^{z+1} \mu(x)dx\right) \quad (48)$$

$$= 1 - \exp\left(-\gamma + \frac{\gamma \log(\delta e^{(\beta x + \beta)} + 1)}{\beta} - \frac{\gamma \log(\delta e^{(\beta x)} + 1)}{\beta} - \frac{\alpha \log(\delta e^{(\beta x + \beta)} + 1)}{\beta \delta} + \frac{\alpha \log(\delta e^{(\beta x)} + 1)}{\beta \delta}\right) \quad (49)$$

$$= 1 - \exp(-\gamma) \left[\frac{\delta \exp(\beta x + \beta) + 1}{\delta \exp(\beta x) + 1} \right]^{\frac{\gamma}{\beta}} \left[\frac{\delta \exp(\beta x) + 1}{\delta \exp(\beta x + \beta) + 1} \right]^{\frac{\alpha}{\beta \delta}} . \quad (50)$$

E.7 Weibull

The Weibull hazard is commonly used in engineering to describe the failure of systems composed of many components; L. A. Gavrilov and Gavrilova (1991) has a good discussion of the Weibull model, though those authors did not recommend it as a model of human mortality.

Hazard function

The Weibull hazard has the form

$$\mu(z) = \alpha z^{\beta-1}. \quad (51)$$

See, for example, K. G. Manton et al. (1986).

Parameters

model	code
$\alpha \in (0, \infty)$	$\exp(\theta_1)$
$\beta \in (0, \infty)$	$\exp(\theta_2)$

Table 11: The parameterization of the Weibull hazard used in the `mortfit` package.

Starting values

In order to compute starting values for the BFGS optimization method, we fit a regression of the log of the central death rates on the log of age; that is, we fit

$$\log(M_z) = a + b \log(z). \quad (52)$$

We then use $\alpha_0 = a$ as the initial estimate of α , and $\beta_0 = \log(b) - 1$ as the initial estimate of β .

Conditional probability of death

$${}_1q_z = 1 - \exp\left(-\int_z^{z+1} \mu(x) dx\right) = 1 - \exp\left(\frac{\alpha}{\beta} \left(z^\beta - (z+1)^\beta\right)\right). \quad (53)$$

E.8 Log-Quadratic

This hazard function is interesting in part because it can produce hazards that decelerate at oldest ages, but it is not logistic. It has been studied by several authors, including Horiuchi (2003) and Steinsaltz and Wachter (2006).

Hazard function

The log-quadratic hazard function has the form

$$\mu(z) = \exp(\alpha + \beta z + \gamma z^2). \quad (54)$$

Parameters

model	code
$\alpha \in (-\infty, \infty)$	θ_1
$\beta \in (-\infty, \infty)$	θ_2
$\gamma \in (-\infty, \infty)$	θ_3

Table 12: The parameterization of the Log-quadratic hazard used in the `mortfit` package.

Starting values

We fit a regression of the logged crude death rates on age and age squared. The estimated coefficients from that regression are the starting values for the BFGS algorithm.

Conditional probability of death

$${}_1q_z = 1 - \exp\left(-\int_z^{z+1} \mu(x)dx\right) \quad (55)$$

$$= 1 - \exp\left(\frac{\sqrt{\pi}\operatorname{erf}\left(\frac{2\gamma x + \beta + 2\gamma}{2\sqrt{-\gamma}}\right)e^{\left(\alpha - \frac{\beta^2}{4\gamma}\right)}}{2\sqrt{-\gamma}} - \frac{\sqrt{\pi}\operatorname{erf}\left(\frac{2\gamma x + \beta}{2\sqrt{-\gamma}}\right)e^{\left(\alpha - \frac{\beta^2}{4\gamma}\right)}}{2\sqrt{-\gamma}}\right) \quad (56)$$

$$= 1 - \exp\left(\frac{\sqrt{\pi}e^{\left(\alpha - \frac{\beta^2}{4\gamma}\right)}}{2\sqrt{-\gamma}} \left[\operatorname{erf}\left(\frac{2\gamma x + \beta + 2\gamma}{2\sqrt{-\gamma}}\right) - \operatorname{erf}\left(\frac{2\gamma x + \beta}{2\sqrt{-\gamma}}\right)\right]\right) \quad (57)$$

$$= 1 - \exp\left(\frac{\sqrt{\pi}e^{\left(\alpha - \frac{\beta^2}{4\gamma}\right)}}{2\sqrt{-\gamma}} \left[\operatorname{erf}\left(\frac{\beta + 2\gamma(x+1)}{2\sqrt{-\gamma}}\right) - \operatorname{erf}\left(\frac{\beta + 2\gamma x}{2\sqrt{-\gamma}}\right)\right]\right) \quad (58)$$

where erf is the error function.

E.9 Lynch-Brown

Hazard function

The Lynch-Brown hazard function was developed to naturally parameterize deceleration and compression in mortality hazards (S. M. Lynch and Brown 2001). The Lynch-Brown hazard is given by

$$\mu(z) = \alpha + \beta \arctan\{\gamma(z - \delta)\}. \quad (59)$$

For given values of β, γ the hazard yields the same hazard as with $-\beta, -\gamma$. In order to identify it, S. M. Lynch and Brown (2001) proposes the constraint that $\beta > 0$. We also use this constraint.

Parameters

model	code
$\alpha \in (-\infty, \infty)$	θ_1
$\beta \in (0, \infty)$	$\exp(\theta_2)$
$\gamma \in (0, \infty)$	$\exp(\theta_3)$
$\delta \in (-\infty, \infty)$	θ_4

Table 13: The parameterization of the Lynch-Brown hazard used in the `mortfit` package.

S. M. Lynch and Brown (2001) has a useful explication of the interpretation of each of these parameters. Overall the hazard has a sigmoid shape. α and δ are shape parameters. α shifts the inflection point of the sigmoid shape up and down.

β is a scale parameter, controlling the height of the sigmoid shape. Larger values of β imply a greater range of hazard values across ages.

γ stretches the curve horizontally, with larger values of γ making the hazard traverse the middle range of the sigmoid shape more quickly.

δ indicates the age at which the inflection point of the sigmoid shape is attained. We allow it to be negative, since we parameterize age 80 as $z = 1$ and it's possible that the inflection point could be estimated to be attained before age 80.

Fit details

Table 1 of S. M. Lynch and Brown (2001) shows parameter estimates from the Lynch-Brown hazard fit to data in the US. We choose the baseline year estimates and take the range of reasonable

parameter values to be these plus and minus 3 standard deviations. Since we parameterize age $z = 1$ to be 80 years, we subtract 79 from the reported δ estimates.

Choosing starting values for the BFGS optimization algorithm is not trivial. We have found that the following procedure has yielded good results: first, compute central death rates $M_z = \frac{D_z}{N_z - 0.5D_z}$. As S. M. Lynch and Brown (2001) point out, the β parameter is the maximum value that the hazard attains, scaled by π , so we take the initial value of β to be $\frac{\max_z D_z}{\pi}$.

The δ parameter is the age at which the inflection point occurs; for an initial estimate, we determine the age at which the fitted values from the logistic regression are closest to the midpoint of the observed central death rates, and take δ to be that value.

γ is the slope of the hazard at the inflection point; as a starting value, we use a numerical approximation to the derivative of the fitted logistic curve at age δ .

Finally, we choose α so that we are guaranteed that the hazard is positive over the range of ages we have data for.

Conditional probability of death

$${}_1q_z = 1 - \exp\left(-\int_z^{z+1} \mu(x) dx\right) \tag{60}$$

$$= 1 - \exp\left(-\alpha - \frac{-\beta}{2\gamma} \left[2k_1 \arctan(k_1) - 2k_0 \arctan(k_0) + \log(k_0^2 + 1) - \log(k_1^2 + 1)\right]\right), \tag{61}$$

where we have defined $k_0 = \gamma(z - \delta)$ and $k_1 = \gamma(z - \delta + 1)$.